Lanthanide-Based Coordination Polymers With 1,4-Carboxyphenylboronic Ligand: Multi-Emissive Compounds For Multi-Sensitive Luminescent Thermometric Probes.

Ahmad Abdallah[a], Stéphane Freslon[a], Xiao Fan[a], Amandine Rojo[a], Carole Daiguebonne[a,*], Yan Suffren[a,*], Kevin Bernot[a], Guillaume Calvez[a], Thierry Roisnel[a] and Olivier Guillou[a].

[a] Univ Rennes, INSA Rennes, CNRS, ISCR "Institut des Sciences Chimiques de Rennes", F-35000 Rennes.

* To whom correspondence should be addressed.

ABSTRACT.

Reactions in water of lanthanide chlorides with the sodium salt of 1,4-carboxyphenylboronic acid (Hcpb) lead to two series of isostructural compounds with respective general chemical formulas $[Ln(cpb)_3(H_2O)_2]_\infty$ for Ln = La or Ce and $[Ln(cpbOH)(H_2O)_2 \cdot (cpb)]_\infty$ for Ln = Pr-Lu (except Pm) plus Y. Hetero-lanthanide coordination polymers that are isostructural to the second series have been synthesized and their photo-physical properties have been studied. This study evidences that it is possible to design multi-emissive lanthanide-based coordination polymers that could find their application as multi-gauge luminescent thermometric probes.

INTRODUCTION.

In the last two decades, there was a growing interest for lanthanide-based coordination polymers because of their fascinating crystal structures[1-4] as well as their interesting porosity,[5-8] magnetic[9-11] and optical properties.[12-15] Because of their unique optical properties lanthanide-based coordination polymers can be suitable for potential applications in various fields such as lighting and display,[14, 16-17] chemical sensing,[18] fight against counterfeiting[19-21] or thermometric probes,[22-37] for examples. Some of these applications require the use of hetero-lanthanide coordination polymers whose first example has been reported in 1994 by Zhou *et al*.[38] Our group is involved in that field for more than a decade and the search of new ligands that lead to new hetero-lanthanide coordination polymers with original luminescence properties is a continuous concern.[39-44]

This article is devoted to the study of hetero-lanthanide based coordination polymers with 4-carboxyphenylboronic acid (Hcpb) as ligand (Scheme 1). This ligand has been chosen because of its rode-like topology, its low toxicity[45] and its ability to behave as both a Lewis and a Bronstëd acids. Moreover, it can act as a structuring ligand via π-stacking and hydrogen bonds. At last, examples of coordination compounds based on boronate ligands are rather scarce[46-47] and, to the best of our knowledge, there is to date only two examples of lanthanide-based coordination polymers with such ligands.[48-49]

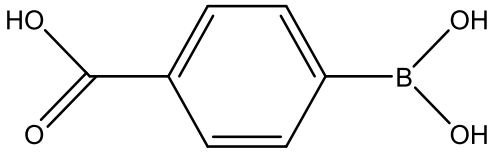

Scheme 1. Schematic representation of the 1,4-carboxyphenylboronic acid hereafter symbolized by Hcpb

EXPERIMENTAL SECTION.

Synthesis and characterization of the starting salts.

1,4-carboxyphenylboronic acid (Hcpb) (>90%) was purchased from Sigma Aldrich and used without any further purification. By recrystallization in water, two different polymorphous phases were isolated depending on the recrystallization process. One out of the two crystal structures was still unknown. It has chemical formula Hcpb·0.25H_2O. Its crystal and final structure refinement data as well as projection views of the asymmetric unit and of the crystal packing are reported in Table S1 and Figures S1 and S2 respectively. Crystal structure of Hcpb has been reported previously (CCDC-247776).[50] This very rich polymorphic system (four different crystal structures reported to date) confirms that this ligand is able to provide various structuring intermolecular interactions (Table 1). Powder diffraction diagram and thermal analysis of the commercial microcrystalline powder revealed that it is isostructural to Hcpb (Figures S3 and S4).

Table 1. Cell parameters for Hcpb·nH_2O with n = 0, 1 or 0.25

	Hcpb	Hcpb·H_2O	Hcpb·0.25H_2O	Hcpb·0.25H_2O
reference	50	50	50	This work
formula	$C_7H_7BO_4$	$C_7H_9BO_5$	$C_7H_{7.5}BO_{4.25}$	$C_7H_{7.5}BO_{4.25}$
system	monoclinic	orthorhombic	orthorhombic	monoclinic
space group (n°)	*C2/c* (15)	*Ccc2* (37)	*Fddd* (70)	*C2/c* (15)
a (Å)	11.378(5)	7.566(5)	13.140(3)	18.226(2)
b (Å	9.825(5)	11.929(7)	18.138(5)	13.2209(17)
c (Å)	7.245(3)	9.769(6)	25.328(7)	15.6353(17)
β (°)	120.08(7)	-	-	125.655(3)
V (Å^3)	700.8(6)	881.7(9)	6037(3)	3061.3(6)
Z	4	4	32	16

Sodium salt of 1,4-carboxyphenylboronic acid was prepared by addition of one equivalent of sodium hydroxide to a suspension of the acid in water. The pH was then adjusted to 9 by another addition of sodium hydroxide to the mixture. The obtained clear solution was then evaporated to dryness and the resulting solid washed with ethanol. Precipitation occurred after ethoxyethane addition. The precipitate was then filtered and dried

in air. The yield was about 90%. Thermal analyses show that the salt is Nacpb·1.5H_2O (Figure S5).

Some single crystals suitable for single crystal X-ray diffraction analysis were obtained by recrystallization in water. In this crystal structure the sodium salt is twice hydrated (Nacpb·2H_2O). Crystal and final structure refinement data as well as a projection view of the asymmetric unit are reported in Table S2 and Figure S6.

Lanthanide oxides (4N) were purchased from AMPERE Company and used without further purification. Lanthanide chlorides were prepared according to established procedures.[51]

Synthesis of the lanthanide-based coordination polymers as microcrystalline powders.

Homo-lanthanide based coordination polymers were obtained by mixing stoichiometric amounts of a lanthanide chloride and the sodium salt of 1,4-carboxyphenylboronic acid in water under ambient pressure and temperature. Precipitation immediately occurred. Precipitates were filtered, rinsed with water and dry in air. The yields were close to 90%. On the basis of their powder X-ray diffraction diagrams, microcrystalline powders were classified in two families of isostructural compounds depending on the involved lanthanide ion (Figure S7): compounds with general chemical formula $[Ln(cpb)_3(H_2O)_2]_\infty$ (hereafter abbreviated as $[Ln(cpb)_3]_\infty$) were obtained for Ln = La or Ce, while for Ln = Pr-Lu (except Pm) plus Y, compounds have general chemical formula $[Ln(cpbOH)(H_2O)_2\cdot(cpb)]_\infty$ that is hereafter abbreviated as $[Ln(cpbOH)]_\infty$. Crystal structure of compounds that constitute the former family is described hereafter. Crystal structure of compounds of the latter family have previously been described.[48]

Hetero-lanthanide based coordination polymers were synthesized according to the same procedure simply replacing the lanthanide chloride solution by a mixture of lanthanide

chlorides solution. All hetero-lanthanide compounds have been assumed to be isostructural to $[Tb(cpbOH)]_\infty$[48] on the basis of their powder X-ray diffraction diagrams (Figures S8 to S14). For all of them, relative contents of the different lanthanide ions have been estimated by EDS measurements (Table S3). On the basis of previous ^{89}Y solid state NMR spectroscopy studies realized on similar compounds,[42-43, 48, 52] it has been assumed that lanthanide ions are randomly distributed over all the metallic sites of the crystal structure.

Crystal growth of the single crystals of $[La(cpb)_3]_\infty$.

Tetramethylorthosilicate (TMOS) was purchased from Acros Organics and jellified according to established procedures.[53-55]

Aqueous solutions of a lanthanum chloride in one hand and of the sodium salt of 1,4-carboxyphenylboronic acid in the other hand were allowed to slowly diffuse through a TMOS gel (7.5% in weight) in a U-shaped tube. After a few weeks, needle-like single crystal suitable for X-ray diffraction were collected and sealed in capillaries in order to avoid any potential dehydration.

Single crystal X-ray diffraction.

Single crystals were mounted on a Nonius Kappa CCD Bruker diffractometer for $[La(cpb)_3]_\infty$ and on a D8 Venture Bruker diffractometer for the other compounds. Crystal data collections were performed with MoK_α radiation ($\lambda = 0.70713$ Å) at room temperature for $[La(cpb)_3]_\infty$ and $Nacpb{\cdot}2H_2O$, and at 150 K for the other compound. Crystal structures were solved by direct methods using the SIR97 program[56] and then refined with full matrix least-squares methods based on F^2 (SHELX97)[57] with the aid of WINGX program.[58] All non-hydrogen atoms were refined anisotropically using the SHELXL program. Hydrogen atoms bound to the organic ligand were located at ideal positions except those of the $-B(OH)_3$

groups in $[La(cpb)_3]_\infty$ crystal structure. Hydrogen atoms of water molecules were not localized. Absorption correction were performed using WinGX program facilities.[58-59] Full details of the X-ray structure determination of the crystal structures of $Hcpb \cdot 0.25H_2O$, of $Nacpb \cdot 2H_2O$ and of $[La(cpb)_3]_\infty$ have been deposited with the Cambridge Crystallographic Data Center under the depositary numbers CCDC-1843158, CCDC-1843156 and CCDC-962509 respectively.

Powder X-ray diffraction.

Experimental diagrams have been collected with a Panalytical X'pert Pro diffractometer equipped with an X'Celerator detector(45 kV, 40 mA for CuK_α (λ = 1.542Å) in θ/θ mode). Calculated diagrams were produced using the Powdercell and WinPLOTR software programs.[60-62]

Optical measurements.

Luminescence spectra (emission and excitation) have been realized on a Horiba Jobin-Yvon Fluorolog III fluorescence spectrometer. This device has been equipped with a Xe lamp 450 W, an UV-Vis photomultiplier (PMT Hamamatsu R928, sensitivity range = 190-860 nm) and an infrared-photodiode cooled by liquid nitrogen (InGaAs, sensitivity range = 800-1600 nm). Classical emission and excitation have been measured on the solid state at room temperature. Quantum yields were measured using a integrating sphere from Jobin-Yvon company thanks to the following formula : $\Phi = (E_c-E_a)/(L_a-L_c)$ (E_c and L_c are the integrated emission spectrum and the absorption at the excitation wavelength of the sample, while E_a and L_a are the integrated “blank” emission spectrum and “blank” absorption, respectively). Quantum yield recordings and emission/excitation spectra were performed on powder samples introduced in cylindrical quartz cells of 2.4 cm height and 0.7 cm diameter,

which were placed inside the integrating sphere. For the IR emissions, powder samples were pasted on copper plates with silver glue or introduced directly in quartz capillary tubes. The Gd-based phospho-luminescence has been realized at 77 K, the powder was placed in a quartz capillary tube, which was introduced inside a small Dewar filled by liquid nitrogen. Emissions and excitations at variable temperature were performed with an optical cryostat coupled with an external liquid nitrogen bath, able to reach temperature of 77 K under nitrogen gas media. Luminescence decays were measured at room-temperature using a Xenon flash lamp (phosphorescence mode) from the Fluorolog III spectrometer. Quantum yields and luminescence decays are averages of two or three independent determinations.

Comparative solid state luminescent spectra have been measured on powders samples shaped into pellets using the Fluorolog III fluorescence spectrometer between 450 and 725 nm under identical operating conditions. The Xenon lamp was maintained switch on during all the measurements to ensure a valid comparison between the emission spectra.

For all the measurements recorded, the residual excitation laser light, the Rayleigh scattered light and associated harmonics from spectra (emission, excitation, decay, quantum yield) were removed with appropriate filters. All spectra were corrected for the instrumental response function.

Luminescence intensities (in $Cd.m^{-2}$) of the powders have been measured using a Gigahertz-Optik X1-1 optometer (integration time = 200 ms) on 1.5 cm^2 pellets under UV irradiation (λ_{exc} = 312 nm). The UV flux (in $mW.cm^{-2}$) at sample location has been measured using a VilberLourmat VLX-3W radiometer. $[Tb_2(bdc)_3 \cdot 4H_2O]_\infty$ compound where bdc^{2-} stands for terephthalate was used as a reference. Its luminance value is 107 $Cd.m^{-2}$ under 312 nm irradiation and a flux of 0.793 $mW.cm^{-2}$.[43]

Solution and solid state UV-visible absorption spectra have performed using a Perkin Elmer Lambda 650 spectrometer equipped with a 60 mm integrated sphere.

Colorimetric measurements.

The CIE (Commission Internationale de l'Eclairage: 2°, CIE 1931, step 5 nm) (x, y) emission color coordinates[63-64] were measured using a MSU-003 colorimeter with the PhotonProbe 1.6.0 Software from Majantys. Color measurements were realized under 312 nm UV light: $X = k \times \int_{380nm}^{780nm} I_\lambda \times x_\lambda$, $Y = k \times \int_{380nm}^{780nm} I_\lambda \times y_\lambda$ and $Z = k \times \int_{380nm}^{780nm} I_\lambda \times z_\lambda$ with k constant for the measurement system, I_λ sample spectrum intensity wavelength depending, x_λ, y_λ, z_λ trichromatic values x = X/(X+Y+Z), y = Y/(X+Y+Z) and z = Z/(X+Y+Z). Mean xyz values are given for each sample, which act as light sources (luminescent samples). Standards from Phosphor Technology were used for calibration at 312 nm: red phosphor Gd_2O_2S:Eu (x = 0.667, y = 0.330) and green phosphor Gd_2O_2S:Tb (x = 0.328, y = 0.537).

Thermal analyzes.

Thermal analyzes were performed with a Perkin-Elmer STA6000 TG/DSC analyzers in the 20-900°C temperature range under N_2 atmosphere in ceramic crucibles.

Electronic microscopy and Energy Dispersive Spectroscopy (EDS).

EDS measurements have been performed with a Hitachi TM-1000 Tabletop Microscope version 02.11 (Hitachi High-Technologies, Corporation Tokyo Japan) with EDS analysis system (SwiftED-TM, Oxford Instruments Link INCA). Samples were deposited on carbon discs pasted on an aluminium stub located at 7 mm from EDX beam, with an angle of measurement of 22°. Reproducibility of the elemental analyses has been checked by repeating the measurements several times. These experiments support the homogeneity of the samples.

RESULTS AND DISCUSSION.

Reactions in water of lanthanide chlorides and the sodium salt of 1,4-carboxyphenylboronic lead to two families of isostructural compounds depending on the involved lanthanide ion: $[Ln(cpb)_3]_\infty$ with Ln = La-Ce and $[Ln(cpbOH)]_\infty$ with Ln = Pr-Lu (except Pm) plus Y (Figure S7).

Crystal structures of $[Ln(cpb)_3]_\infty$ with Ln = La-Ce.

La^{3+}- and Ce^{3+}-based coordination polymers have general abbreviated chemical formula $[Ln(cpb)_3]_\infty$ where Ln = La or Ce. Crystal structure has been solved on the basis of the lanthanum-containing derivative. Crystal and final structure refinement data of the crystal structure are listed in Table 2.

Table 2. Crystal and final structure refinement data for $[La(cpb)_3]_\infty$

Molecular formula	$La_1C_{21}H_{22}B_3O_{14}$
System	monoclinic
Space group (No.)	$P2_1/n$ (14)
a (Å)	22.7993(5)
b (Å)	5.2334(1)
c (Å)	23.2460(6)
β (°)	118.608(1)
V (Å^3)	2435.04(10)
Z	4
Formula weight (g.mol^{-1})	669.73
D_{calc} (g.cm^{-3})	1.827
μ (mm^{-1})	1.828
R (%)	4.63
R_W (%)	11.80
GoF	1.230
N° CCDC	962509

The crystal structure can be described as the superimposition of one dimensional double-chains molecular motifs that spread along the *b* axis. Molecular motifs are held together by a strong hydrogen-bonds network that involves -OH groups of the boronic functions ($d_{O\text{-}O} \approx 2.77$ Å) in one hand and the coordination water molecules ($d_{O\text{-}O} = 2.84$ Å) in the other hand (Figure 1).

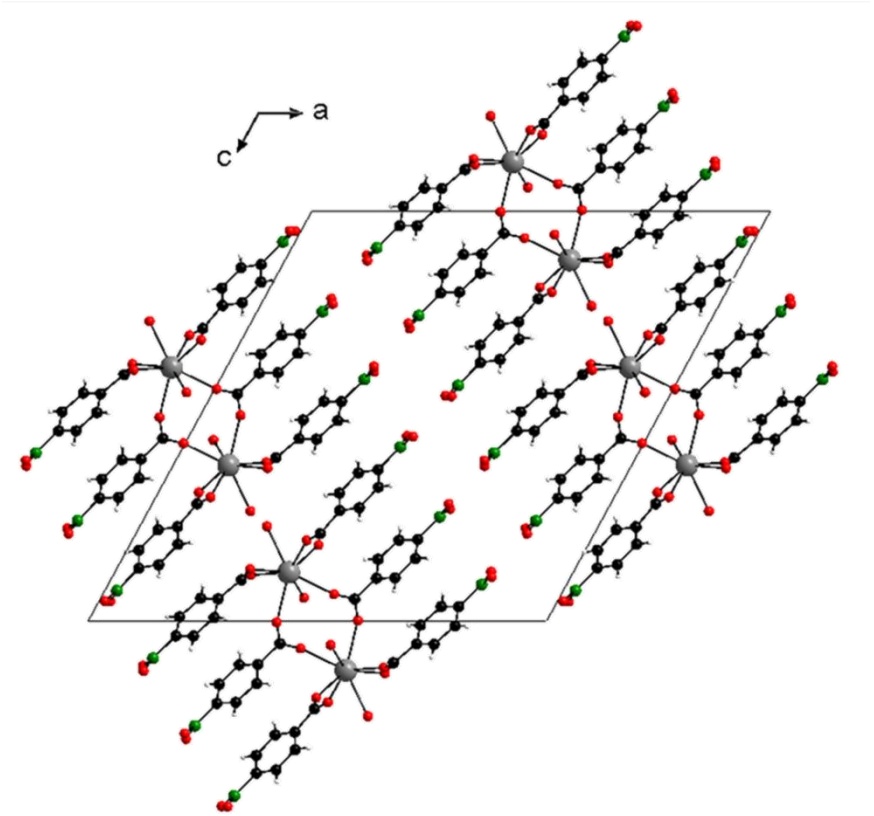

Figure 1. Projection view along the *b* axis of an extended unit cell of $[La(cpb)_3]_\infty$.

There is only one independent La^{3+} ion in the crystal structure. It is eight-coordinated by six oxygen atoms from six carboxylate functions from different cpb^- ligands and by two oxygen atoms from coordination water molecules that generate a bi-augmented trigonal prism (C_{2v} site symmetry). There are three independent cpb^- ligands but all three adopt the same bridging coordination mode (Figure 2): the carboxylate function links two different La^{3+} ions in a unidentate manner while the boronic function is free and only involved in the inter-chains hydrogen-bonds network.

From a global point of view, there are two different types of ligands: Type **A** that links lanthanum ions along the *b* direction and form two linear chains that spread parallel to the *b* axis and type **B** that binds lanthanum ion that belong to different chains (See Figure 2).

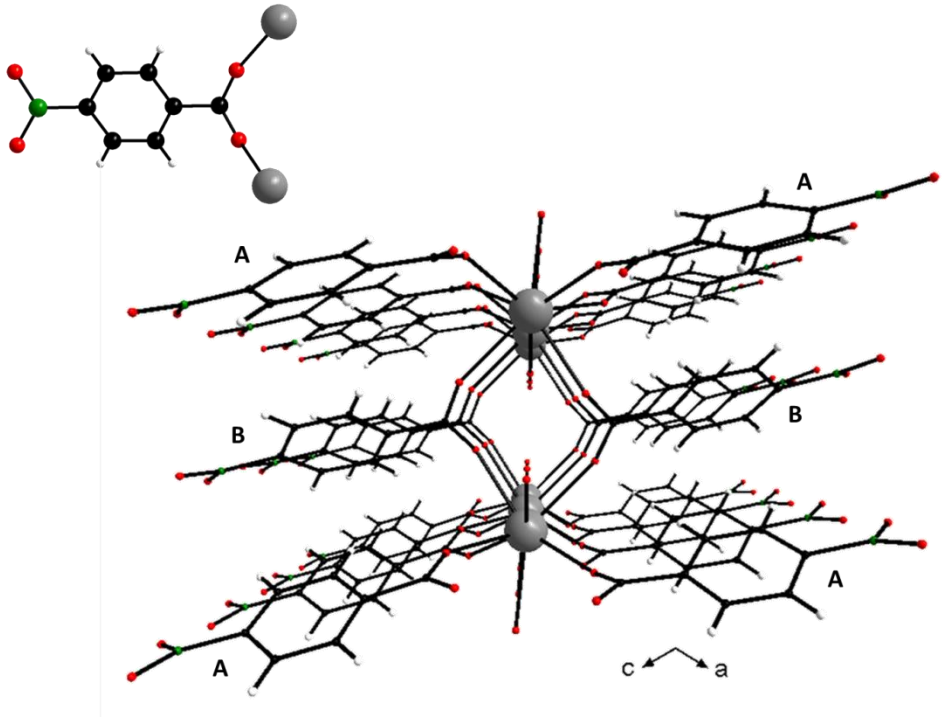

Figure 2. Perspective view along the *b* axis of a double-chains molecular motif in $[La(cpb)_3]_\infty$. In inset, coordination mode of the cpb^- ligands in $[La(cpb)_3]_\infty$.

Crystal structures of $[Ln(cpbOH)]_\infty$ with Ln = Pr-Lu (except Pm) plus Y.

Coordination polymers that are obtained with one of the rare earth comprised between praseodymium and lutetium (except promethium) or yttrium are all isostructural with $[Tb(cpbOH)]_\infty$ whose crystal structure has been reported previously (CCDC-962513).[48] Its crystal structure is two-dimensional and can be described on the basis of wavy planes that spread parallel to the *ab* plane. In the inter-planes space isolated cpb^- ligands insure the electro-neutrality of the crystal packing (See figure 3).

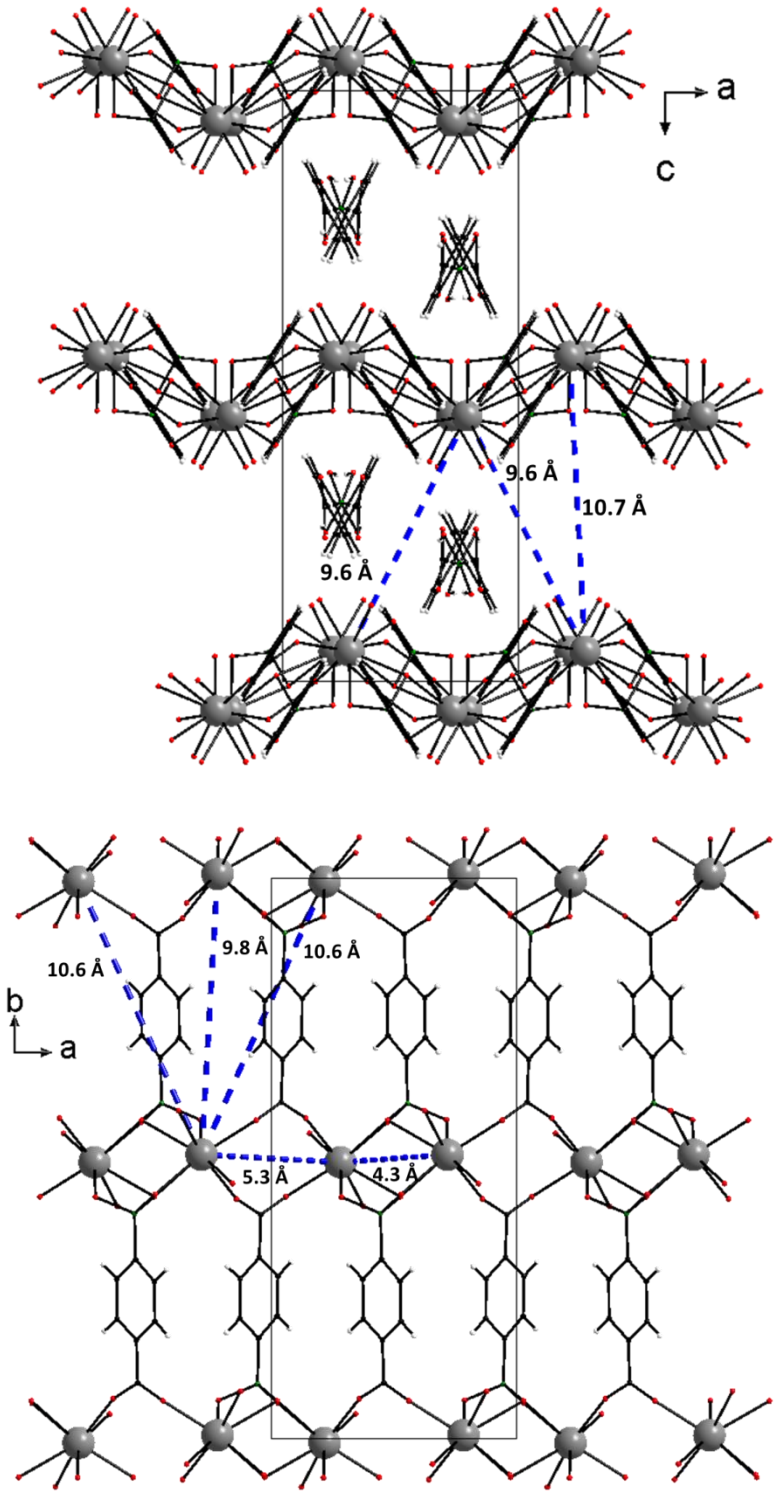

Figure 3. Top: Projection view along the *b* axis of the crystal packing of $[Tb(cpbOH)]_{\infty}$. Shortest intermetallic distances between lanthanide ions that belong to different wavy planes are reported. Bottom: Projection view along the *c* axis of a molecular wavy plane in $[Tb(cpbOH)]_{\infty}$. Shortest intermetallic distances are reported. This compound crystallizes in the orthorhombic system, space group *Pbca* (n°61) with a = 8.5704(1) Å, b = 19.5441(1) Å and c = 21.4191 Å (CCDC-962513). Redrawn from reference 48.

As far as luminescent properties are targeted, this second family of compounds is the most interesting one because it contains all the lanthanide ions that can emit in the visible or NIR regions. As a consequence, intermetallic distances between lanthanide ions have to be carefully considered because they influence intermetallic energy transfers efficiency. In this crystal structure, chains of lanthanide ions spread along the *a* axis. In these chains, the shortest distances between neighboring lanthanide ions are 5.3 Å and 4.3 Å. These chains are bound to each other by cpb^- ligands to form wavy molecular planes. The shortest distances between lanthanide ions that belong to neighboring chains are 9.8 Å. Last, the shortest distances between lanthanide ions that belong to different wavy planes are 9.6 Å. For estimating the mean distance between lanthanide ions in the crystal structure, it is possible to use the rough model that has already been used successfully previously.[65] In this model, the mean volume occupied by a lanthanide ion is calculated as the cell volume (3588 $Å^3$) divided by the number of lanthanide ions in the unit cell ($Z = 8$). This mean volume corresponds to a sphere with a 4.75 Å radius which suggests that the mean distance between two lanthanide ions is roughly 9.5 Å which. Therefore, according to this model, a dilution by 10% of the optically active lanthanide ions would reduce significantly inter-metallic energy transfers. Indeed, it is usually considered that inter-metallic energy transfers become less efficient when there is no acceptor lanthanide ion closer than 10 Å from a given lanthanide ion.[66-67] This can be achieved by dilution of optically active lanthanide ions by non-acceptor lanthanide ions (such as Gd^{3+}, Y^{3+} or Lu^{3+} for instance).

However, Scheme 2 shows that the 9.5 Å mean inter-metallic distance is overestimated in the present case. Indeed, it does not reflect the anisotropic character of the lanthanide ions distribution in the crystal structure. Actually, from a global point of view, for a given lanthanide ion, eight other lanthanide ions are closer than 10 Å and two out of the eight are much closer (4.3 - 5.3 Å) than the six others (9.6 - 9.8 Å) (Figure 3). Therefore a

dilution by more than 50% is necessary for embedding energy transfers between neighboring lanthanide ions that belong to the same molecular chain and a dilution of almost 90% for insuring insulation of a given lanthanide ion from other acceptor lanthanide ions.

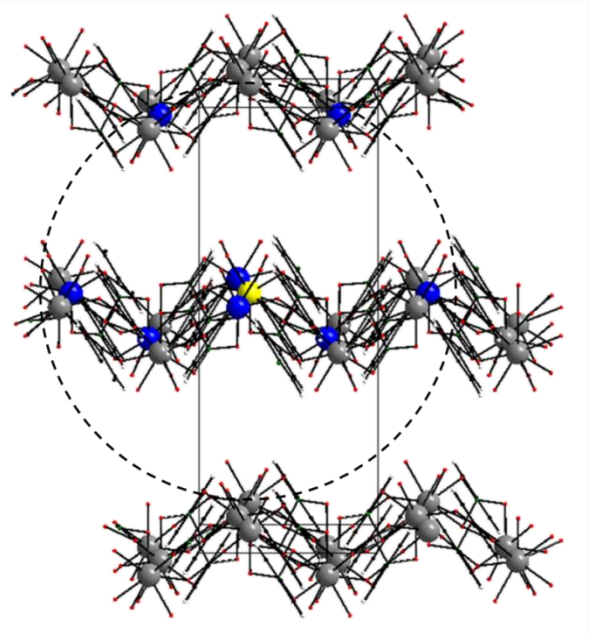

Scheme 2. Representation of the neighborhood of a given lanthanide ion (in yellow). Lanthanide ions that are closer than 10 Å from that given lanthanide ion, are in blue. Dotted line represents the projection of a virtual sphere centered on the given lanthanide ion (in yellow) and with a 10 Å radius.

Solid state luminescence properties of homo-lanthanide coordination polymers $[Ln(cpbOH)]_\infty$ with Ln = Nd, Sm, Eu, Gd, Tb, Dy, or Ho.

Energies of the lowest excited singlet and triplet states of the ligand have been estimated by referring respectively to the wavelength of the excitation edge ($E\ ^1\pi-\ ^1\pi^* = 325$ nm = 30750 cm^{-1}) and to the shortest wavelength phosphorescent band ($E\ ^1\pi-\ ^3\pi^* = 400$ nm = 25000 cm^{-1}) of $[Gd(cpbOH)]_\infty$ (Figure S15).[68-70]

According to Reinhoudt's empirical rule, the intersystem crossing process becomes effective when ΔE ($^1\pi\pi^*$-$^3\pi\pi^*$) is at least 5000 cm^{-1}.[71] In this compound, the gap between the singlet and the triplet exited state (5750 cm^{-1}) is favorable for an efficient intersystem crossing process.

Solid-state luminescent properties have been recorded in visible or near IR regions for $[Ln(cpbOH)]_\infty$ with Ln = Nd, Sm, Eu, Tb, Dy and Ho. These measurements show that an antenna effect[72] is observed for all the compounds. Most emitting homo-lanthanide compounds are those which are based on Nd^{3+}, Eu^{3+} or Tb^{3+} (Figure 4). This is in agreement with Latva's empirical rule[73] that predicts that the energy of the first excited triplet state (25000 cm^{-1}) allows good ligand-to-metal energy transfer without significant back transfer for Tb^{3+} ($^5D_4 \rightarrow {}^7F_{6\text{-}0}$ transitions) and Eu^{3+} ($^5D_0 \rightarrow {}^7F_{0\text{-}4}$ transitions). Despite its low luminescent energy level, an antenna effect is also observed for the Nd^{3+}-based compound ($^4F_{3/2} \rightarrow {}^4I_{9/2}$, $^4I_{11/2}$, $^4I_{13/2}$ transitions) (Scheme 3).

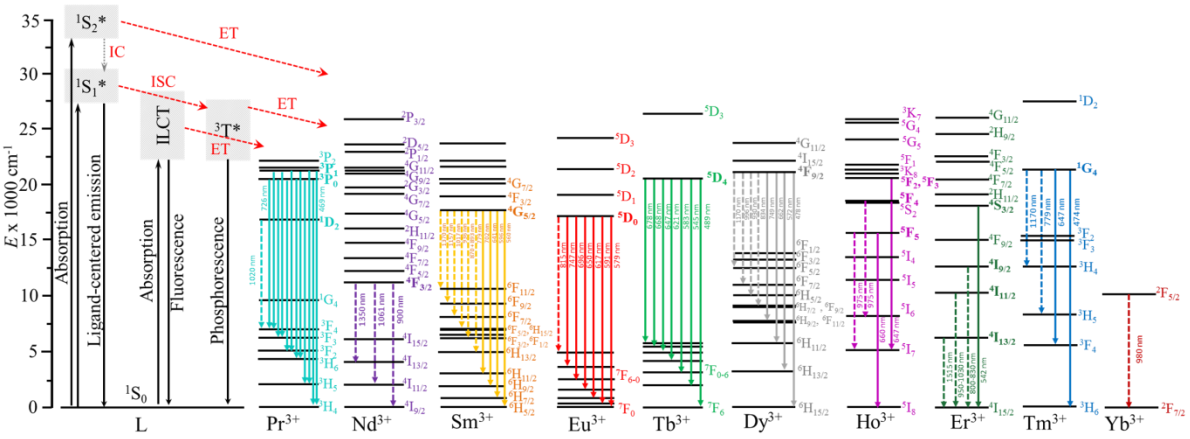

Scheme 3. Simplified Dieke-Jablonsky diagram for emissive lanthanide ions.

Excitation and emission spectra of $[Ln(cpbOH)]_\infty$ with Ln = Sm^{3+}, Dy^{3+} or Ho^{3+} are reported in (Figure S16). Their weak luminescence can be related to their small energy gaps.[74] Overall luminescent quantum yields and observed lifetime for both the Eu- and the Tb-based homo-lanthanide compounds have been measured. They are reported in Table 3. These results complete and confirm previously reported results about Tb- and Eu-derivatives.[48]

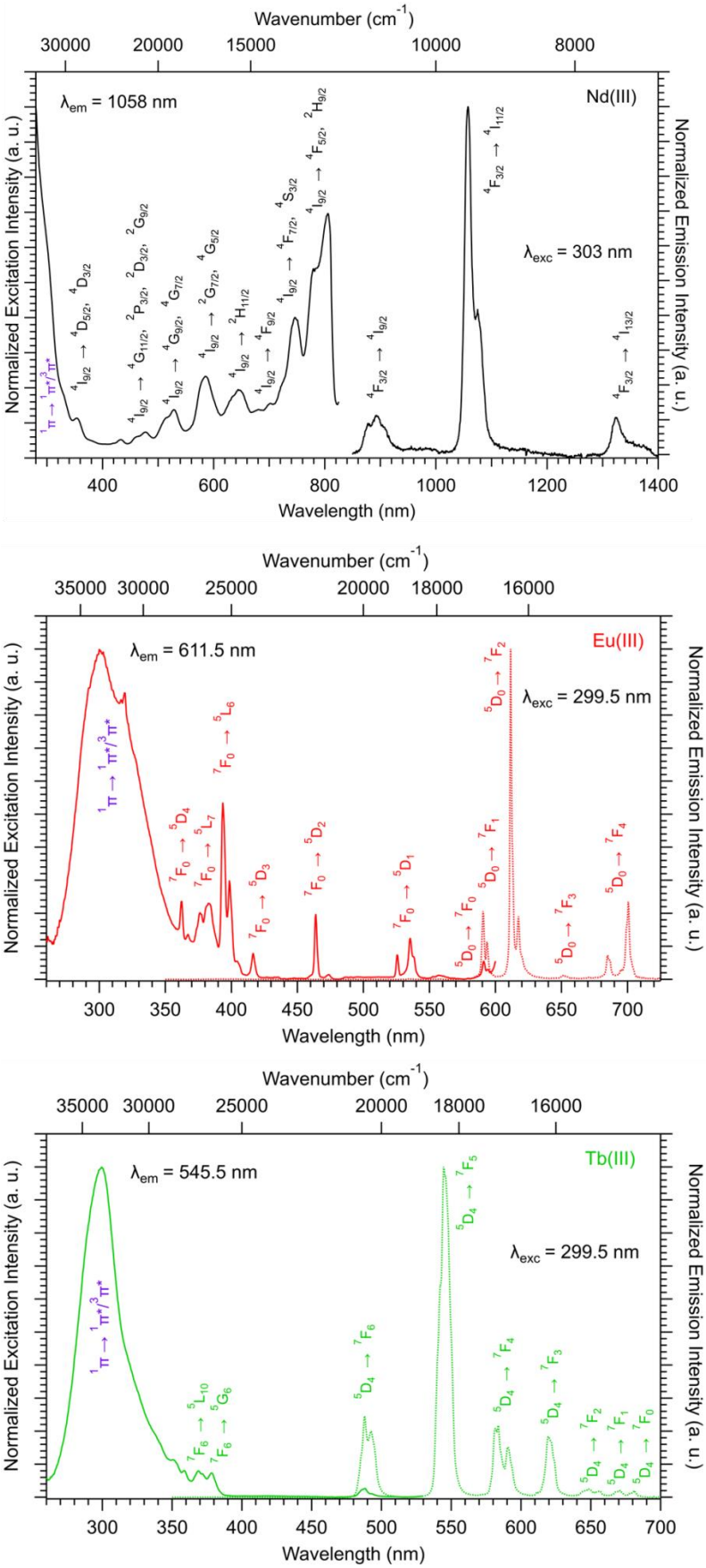

Figure 4. Solid state excitation and emission spectra of $[Ln(cpbOH)]_{\infty}$ with Ln = Nd(III), Eu(III) or Tb(III) at 293 K.

Table 3. Overall luminescent quantum yields and observed lifetime for $[Ln(cpbOH)]_\infty$ with Ln = Eu and Tb

	$Q_{Ln^{3+}}^{Ligand}$ (%)	τ_{obs} (ms)
$[Eu(cpbOH)]_\infty$	6.4(3)	0.27(1)
$[Tb(cpbOH)]_\infty$	39(1)	0.83(1)

Solid state luminescence *versus* temperature of $[Ln(cpbOH)]_\infty$ with Ln = Nd, Eu or Tb.

Because thermometric probe application is targeted, dependence upon temperature of solid state luminescence of the three most luminescent homo-nuclear compounds has been studied in the 77 K - 293 K range (Figure 5). In the following, luminescence intensity of a given lanthanide ion will be assumed to be proportional to the integrated intensity of the most intense characteristic emission peak of this lanthanide ion, that is the one centered at 544.5 nm for Tb^{3+} ($^5D_4 \rightarrow {}^7F_5$), the one centered at 611.5 nm for Eu^{3+} ($^5D_0 \rightarrow {}^7F_2$) and the one centered at 1055 nm for Nd^{3+} ($^4F_{3/2} \rightarrow {}^4I_{11/2}$). It will be symbolized hereafter by I_{Ln}.

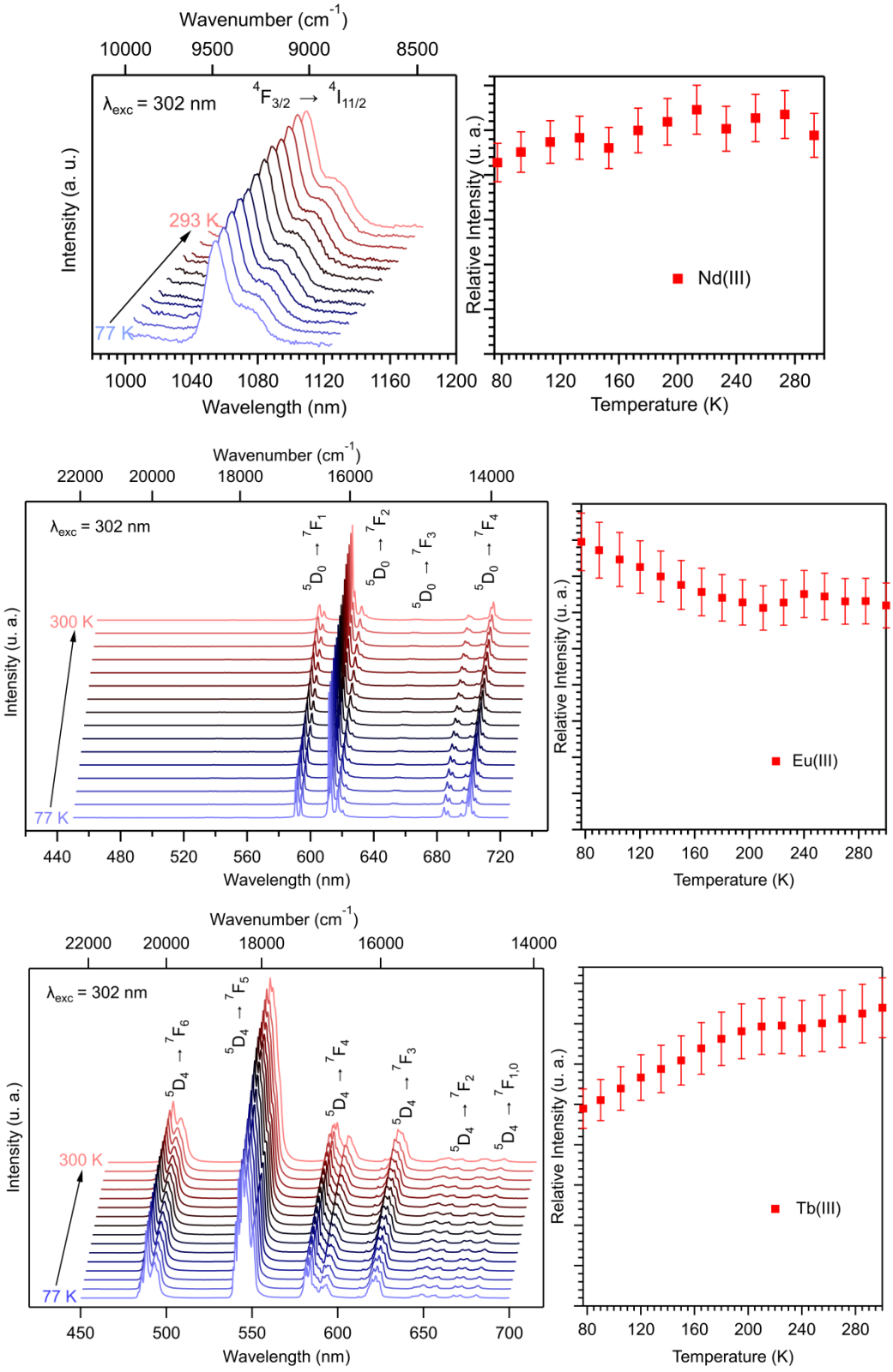

Figure 5. Left: Luminescence spectra *versus* temperature of $[Ln(cpbOH))]_{\infty}$ with Ln = Nd (Top), Eu (Middle) or Tb (Bottom). λ_{exc} = 302 nm. Right: Integrated intensity I_{Ln} *versus* T for the three compounds.

Figure 5 shows that luminescence of homo-nuclear Nd^{3+}-based compound is only weakly influenced by temperature while the one of the homo-nuclear Eu^{3+}-based compound decreases when temperature increases. This decreasing is not surprising and can be related to the increasing of vibrational-based non-radiative de-excitation. On the opposite, figure 5 evidences that luminescence intensity of the homo-nuclear Tb^{3+}-based compound increases when temperature increases. This behavior is quite rare but have already been observed.[75]

Estimation of the inter-metallic energy transfer efficiency: Emission in the visible region of hetero-lanthanide coordination polymers, $[Tb_{1-x}Gd_x(cpbOH)]_\infty$, $[Eu_{1-x}Gd_x(cpbOH)]_\infty$, $[Tb_{1-x}Eu_x(cpbOH)]_\infty$ with $0 \leq x \leq 1$ and $[Gd_{0.2}Tb_{0.8-x}Eu_x(cpbOH)]_\infty$ with $0 \leq x \leq 0.8$.

Four families of hetero-lanthanide compounds have been synthesized: $[Tb_{1-x}Gd_x(cpbOH)]_\infty$, $[Eu_{1-x}Gd_x(cpbOH)]_\infty$, $[Tb_{1-x}Eu_x(cpbOH)]_\infty$ with $0 \leq x \leq 1$ and $[Gd_{0.2}Tb_{0.8-x}Eu_x(cpbOH)]_\infty$ with $0 \leq x \leq 0.8$. All compounds that constitute these series have been assumed to be iso-structural to $[Tb(cpbOH)]_\infty$ on the basis of their powder diffraction diagrams (Figure S8 to S11). Relative contents of the lanthanide ions have been measured by EDS and they are reported in Table S3. On the basis of previous results obtained on similar systems,[42-43, 52, 76] it has been assumed that lanthanide ions are randomly distributed over the metallic sites of the crystal structure.

In order to estimate the efficiency of intermetallic energy transfers, emission spectra have been measured for all the compounds with general chemical formulas $[Tb_{1-x}Gd_x(cpbOH)]_\infty$ and $[Eu_{1-x}Gd_x(cpbOH)]_\infty$ with $0 \leq x \leq 1$. Results are reported in Figure 6.

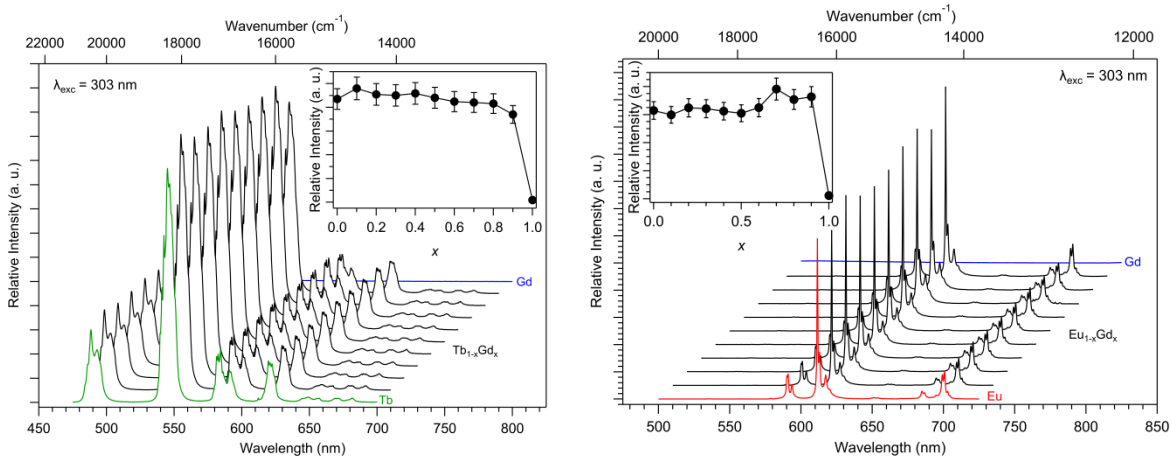

Figure 6. Luminescence spectra of $[Tb_{1-x}Gd_x(cpbOH)]_\infty$ (left) and of $[Eu_{1-x}Gd_x(cpbOH)]_\infty$ (right) with $0 \leq x \leq 1$ *versus* x (λ_{exc} = 303 nm) at 293 K. In insets, integrated intensities of the major characteristic emission peaks of Tb^{3+} centered at 545 nm ($^5D_4 \rightarrow {}^7F_5$) (left) and of Eu^{3+} centered at 611.5 nm ($^5D_0 \rightarrow {}^7F_2$) (right) *versus* x.

For both systems, these measurements are quite different from what is usually observed.[39-44, 65] Actually, as Gd^{3+} content increases, an abrupt increasing of the luminescence intensity is not observed. This is probably related to the very short inter-metallic distances along the *a* crystallographic axis (4.3 - 5.3 Å). Indeed, inter-metallic energy transfer efficiency highly depends on inter-metallic distance[66-67] and it has been demonstrated that presence of "dimeric" units induces very efficient inter-metallic energy transfer even when average inter-metallic distance is important.[77] On the other hand, luminescence intensity is almost unchanged from $x = 0.1$ to $x = 0.8$ which indicates that the decrease of optically active lanthanide ions content (Tb^{3+} or Eu^{3+}) is compensated by the diminution of inter-metallic energy transfer. This suggests that inter-metallic energy transfer is strong and that dilution by non-acceptor lanthanide ion (Gd^{3+}) is efficient over a large range of dilution rate. This is in quite good agreement with the fact that, for a given lanthanide ion there are eight lanthanide ions that are closer than 10 Å in the crystal structure.

In order to estimate Tb^{3+}-to-Eu^{3+} energy transfer, luminescence spectra of $[Tb_{1-x}Eu_x(cpbOH)]_\infty$ with $0 \leq x \leq 1$ have been measured (Figure 7). These measurements shows an efficient Tb^{3+}-to-Eu^{3+} energy transfer as soon as x becomes greater than 0.1. To

quantify the efficiency of this inter-metallic transfer (η_{ET}), luminescence lifetimes of $[Tb_{1-x}Eu_x(cpbOH)]_\infty$ and $[Tb_{1-x}Gd_x(cpbOH)]_\infty$ with $0 \leq x \leq 1$ have been measured and relationship **(1)** has been used (See Table 4):

$$\eta_{ET} = 1 - \frac{\tau_{obs}}{\tau_0} \qquad \textbf{(1)}$$

where τ_{obs} and τ_0 are the observed luminescent lifetimes of Tb^{3+} in presence (τ_{obs}) and in absence (τ_0) of an acceptor ion(Eu^{3+}).[74]

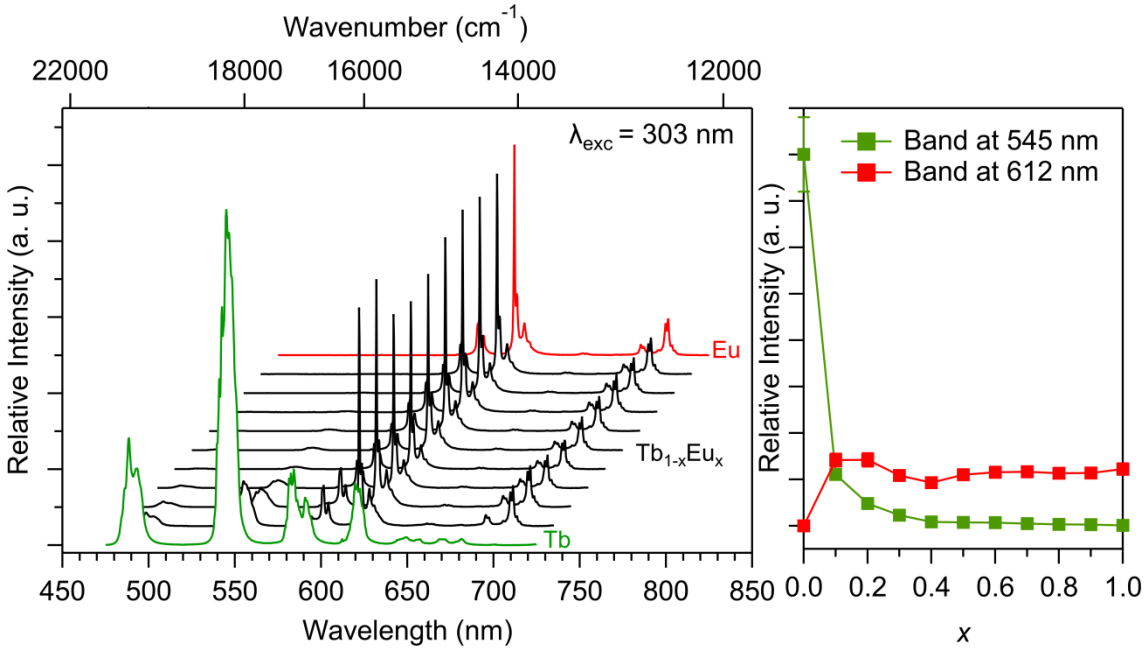

Figure 7. Left: Luminescence spectra of $[Tb_{1-x}Eu_x(cpbOH)]_\infty$ with $0 \leq x \leq 1$ *versus* x (λ_{exc} = 303 nm) at 293 K. Right: integrated intensities of the major characteristic emission peaks of Tb^{3+} and Eu^{3+} centered at 545 nm ($^5D_4 \rightarrow {}^7F_5$) and 612 nm ($^5D_0 \rightarrow {}^7F_2$) respectively *versus x*.

Table 4. Observed lifetimes for $[Tb_{1-x}Eu_x(cpbOH)]_\infty$ and $[Tb_{1-x}Gd_x(cpbOH)]_\infty$ for $0 \leq x \leq 1$

	$[Tb_{1-x}Gd_x(cpbOH)]_\infty$										
x =	0	0.1	0.2	0.3	0.4	0.5	0.6	0.7	0.8	0.9	1
$\tau_{Tb}{}^* = \tau_0$ (ms)	0.83	0.86	0.85	0.85	0.85	0.85	0.85	0.86	0.86	0.86	n/a
	$[Tb_{1-x}Eu_x(cpbOH)]_\infty$										
x =	0	0.1	0.2	0.3	0.4	0.5	0.6	0.7	0.8	0.9	1
$\tau_{Tb}{}^* = \tau_{obs}$ (ms)	0.83	0.57	0.50	0.45	0.43	0.50	0.49	0.48	0.45	0.40	n/a
$\tau_{Eu}{}^*$ (ms)	n/a	0.30	0.26	0.25	0.27	0.27	0.27	0.27	0.27	0.27	0.27
$\eta_{ET}{}^*{}_{(\%)}$	n/a	33	41	47	49	42	43	43	48	54	n/a

* uncertainties on the measurements are evaluated to 5%

Figure 7 and Table 4 show that inter-metallic energy transfer reaches a plateau for $x \approx 0.2$ and then remains almost constant. This quite moderate value of the calculated inter-metallic energy transfer efficiency ($\eta_{ET} \approx 45\%$) was unexpected. Indeed, colorimetric coordinates of $[Tb_{1-x}Eu_x(cpbOH)]_\infty$ (Figure 8) evidence a very efficient Tb^{3+}-to-Eu^{3+} energy transfer that compares well with what was observed in previously reported systems for which η_{ET} was about 90%.[43] This is probably related to the anisotropic character of the metallic distribution in this crystal structure.

In order to estimate the effect of optical dilution in this Eu/Tb system, series of compounds with respective general chemical formulas $[Tb_{1-x}Eu_x(cpbOH)]_\infty$ with $0 \leq x \leq 1$ and $[Gd_{0.2}Tb_{0.8-x}Eu_x(cpbOH)]_\infty$ with $0 \leq x \leq 0.8$ were compared on the basis of their luminance and colorimetric coordinates under UV irradiation, and luminescence spectra (Figure 8). This comparison evidences that dilution by 20% of Gd^{3+} ions reduces significantly inter-metallic energy transfer and allows to observe both characteristic emissions of Tb^{3+} and Eu^{3+} ions under unique UV irradiation.

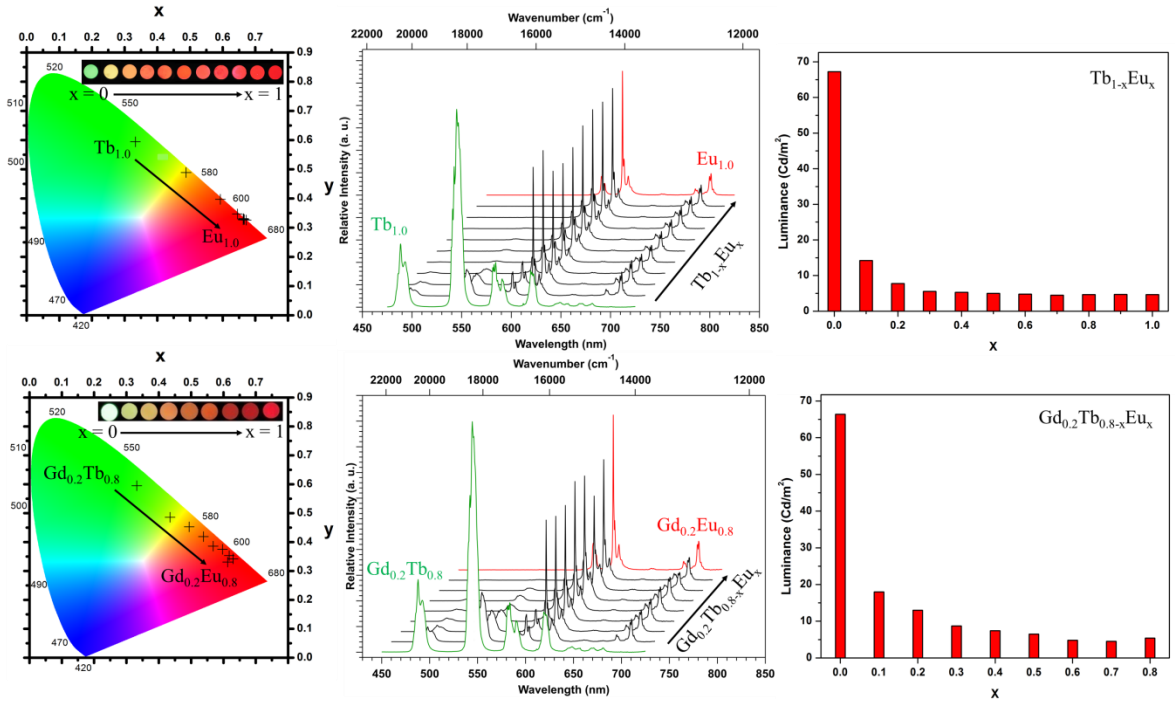

Figure 8. Colorimetric coordinates, luminescence spectra (λ_{exc} = 303 nm) and luminance *versus* *x* under UV irradiation of $[Tb_{1-x}Eu_x(cpbOH)]_\infty$ with $0 \leq x \leq 1$ (Top) and of $[Gd_{0.2}Tb_{0.8-x}Eu_x(cpbOH)]_\infty$ with $0 \leq x \leq 0.8$ (Bottom).

Temperature-dependent emission in the visible region for hetero-lanthanide coordination polymers, $[Tb_{0.5}Eu_{0.5}(cpbOH)]_\infty$ and $[Gd_{0.2}Tb_{0.7}Eu_{0.1}(cpbOH)]_\infty$.

Luminescence spectra of $[Tb_{0.5}Eu_{0.5}(cpbOH)]_\infty$ were recorded between 77 K and 293 K (Figure 9).

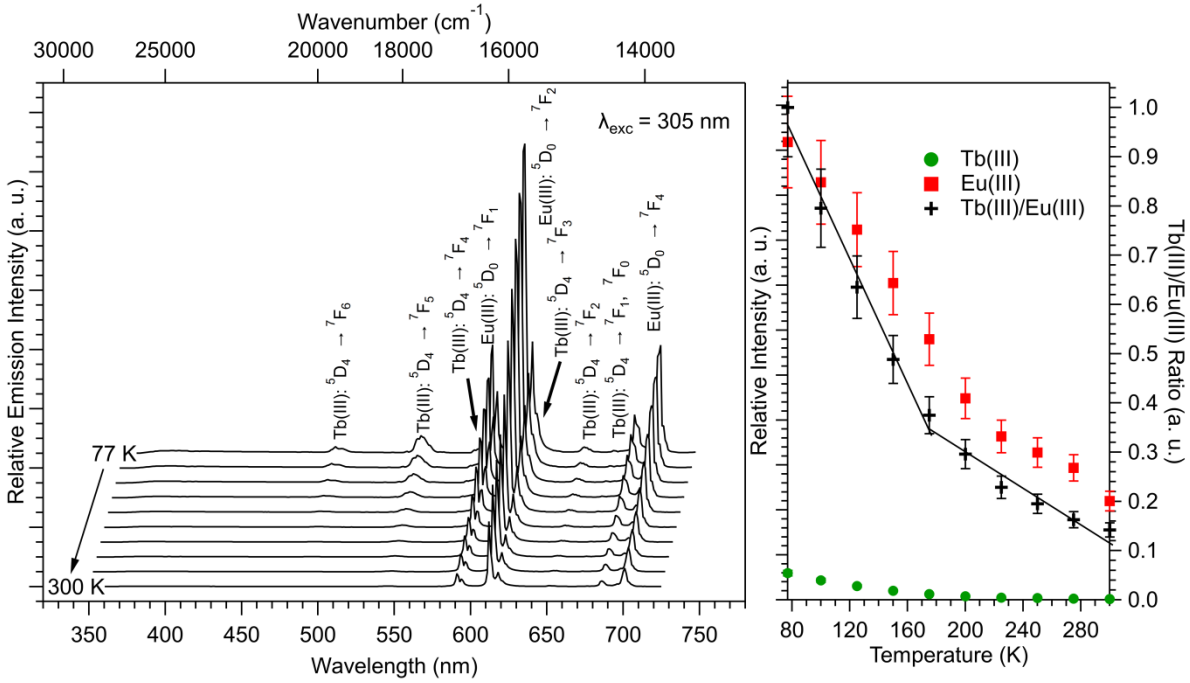

Figure 9. Left: Luminescence spectra of $[Tb_{0.5}Eu_{0.5}(cpbOH)]_\infty$ (λ_{exc} = 305 nm) between 77 and 293 K. Right: Relative intensities of Tb^{3+} (I_{Tb}) and Eu^{3+} (I_{Eu}) and the ratio I_{Tb}/I_{Eu} *vs* temperature.

Figure 9 shows that I_{Tb}/I_{Eu} ratio can be fitted by two linear relationships with quite good agreement factors: between 77 K and 175 K, $I_{Tb}/I_{Eu} = -0.006T + 1.451$ ($R^2 = 0.985$), and between 175 K and room temperature, $I_{Tb}/I_{Eu} = -0.0018T + 0.6676$ ($R^2 = 0.941$).

Evaluation of the sensitivity of molecular thermometers is used to be calculated by the following relationship: [25]

$$S = \frac{\frac{\partial P}{\partial T}}{P} \qquad \textbf{(2)}$$

where P is the temperature dependent parameter that has been chosen (luminescence intensity, luminescence lifetime or luminescence intensity ratio for instance).[25-26] Therefore, in the present case, relationship **(2)** becomes:

$$S = \frac{\frac{\partial(I_{Tb}/I_{Eu})}{\partial T}}{I_{Tb}/I_{Eu}} \qquad \textbf{(3)}$$

With this relationship, the maximum sensitivity for this system is 1.18 %.K^{-1} centered at 130 K in the 77 - 300 K temperature range (Figure S17). This value is in agreement with what has previously been reported for other systems.[29]

However, Figure 9 also evidences that this compound is not optimized as far as thermometer probes are targeted. Indeed, both Eu^{3+} and Tb^{3+} ions, luminescence intensities decrease as the temperature increases. Moreover, variation of Tb^{3+} intensity is moderate and the curve I_{Tb} *vs* T is almost flat. At last, relative luminescence intensity of Tb^{3+} is low ($0\% < I_{Tb}^{normalyzed} < 6\%$) which induces a low accuracy of its determination.

To increase I_{Tb}, optically diluted anologous $[Gd_{0.2}Tb_{0.7}Eu_{0.1}(cpbOH)]_\infty$ was synthesized and its emission spectra were recorded between 77 K and room temperature (Figure 10). As expected, I_{Tb} is much greater ($45\% < I_{Tb}^{normalyzed} < 85\%$) than in the previous compound. Moreover, luminescence intensity of Tb^{3+} and of Eu^{3+} do not vary in the same way anymore: as the temperature increases, Eu^{3+} luminescence intensity slightly oscillates between 77 K and 300 K with a maximum at 160 K and a minimum at 250 K while the one of Tb^{3+} decreases continuously over the whole temperature range.

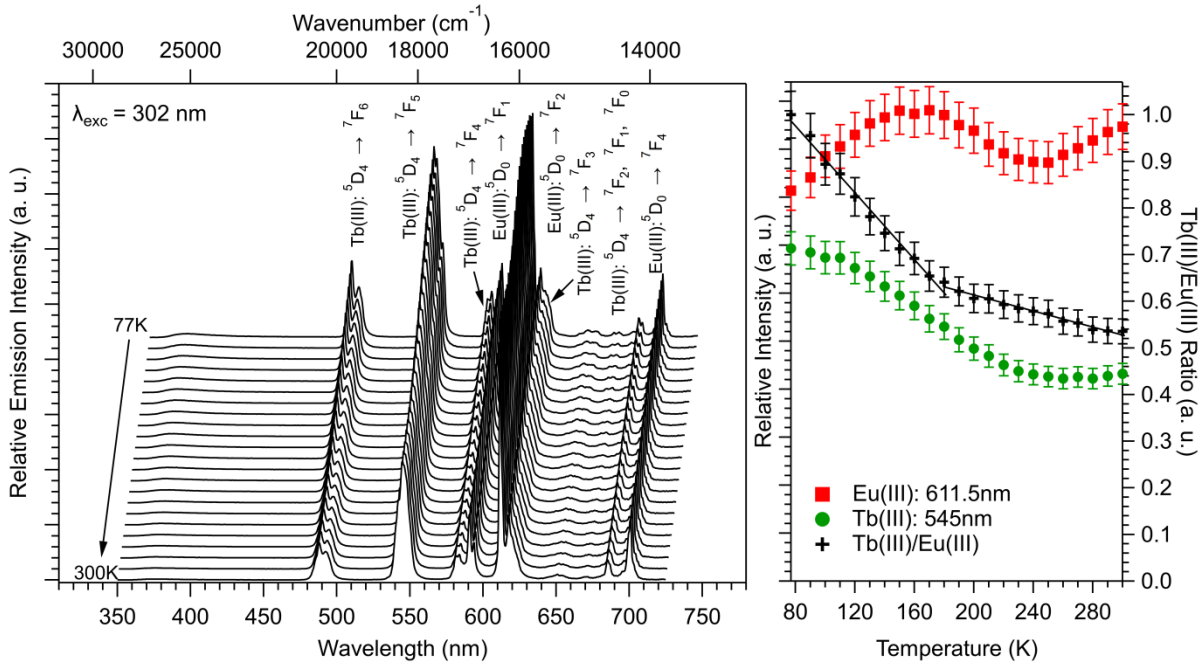

Figure 10. Luminescence spectra of $[Gd_{0.2}Tb_{0.7}Eu_{0.1}(cpbOH)]_\infty$ (λ_{exc} = 302 nm) between 77 and 300 K (left). Relative intensities of Tb^{3+} (I_{Tb}) and Eu^{3+} (I_{Eu}) and the ratio I_{Tb}/I_{Eu} *vs* temperature (right).

Once again, ratio I_{Tb}/I_{Eu} can be fitted by two linear functions depending on the temperature range: from 77 K to 180 K, I_{Tb}/I_{Eu} = -0.0036T + 1.2641 (R^2 = 0.988) and from 180 K to room temperature I_{Tb}/I_{Eu} = -0.0009T + 0.7846 (R^2 = 0.978). Maximum sensitivity is 0.57 %.K^{-1} at 80 K in the 77 - 300 K temperature range (Figure S18). Sensitivity is lower for this new system but accuracy of the measurements is greater.

Emission in the visible and the IR regions of hetero-lanthanide coordination polymers, $[Tb_{0.95}Nd_{0.05}(cpbOH)]_\infty$, $[Gd_{0.2}Tb_{0.75}Nd_{0.05}(cpbOH)]_\infty$, $[Gd_{0.2}Tb_{0.40}Eu_{0.25}Nd_{0.15}(cpbOH)]_\infty$ and $[Eu_{1-x}Nd_x(cpbOH)]_\infty$.

Since inter-metallic energy transfer can be modulated by optical dilution in this system, dual visible and IR emission can be targeted. This is the reason why $[Tb_{0.95}Nd_{0.05}(cpbOH)]_\infty$ and $[Gd_{0.20}Tb_{0.75}Nd_{0.05}(cpbOH)]_\infty$ have been synthesized (Figure S12 and Table S3). Their luminescence spectra were recorded at room temperature (Figure 11). In

both cases, characteristic luminescence of both Tb^{3+} and Nd^{3+} ions was observed. To the best of our knowledge, this is quite rare because most often, the presence of Nd^{3+} provokes a quenching of Tb^{3+} luminescence.

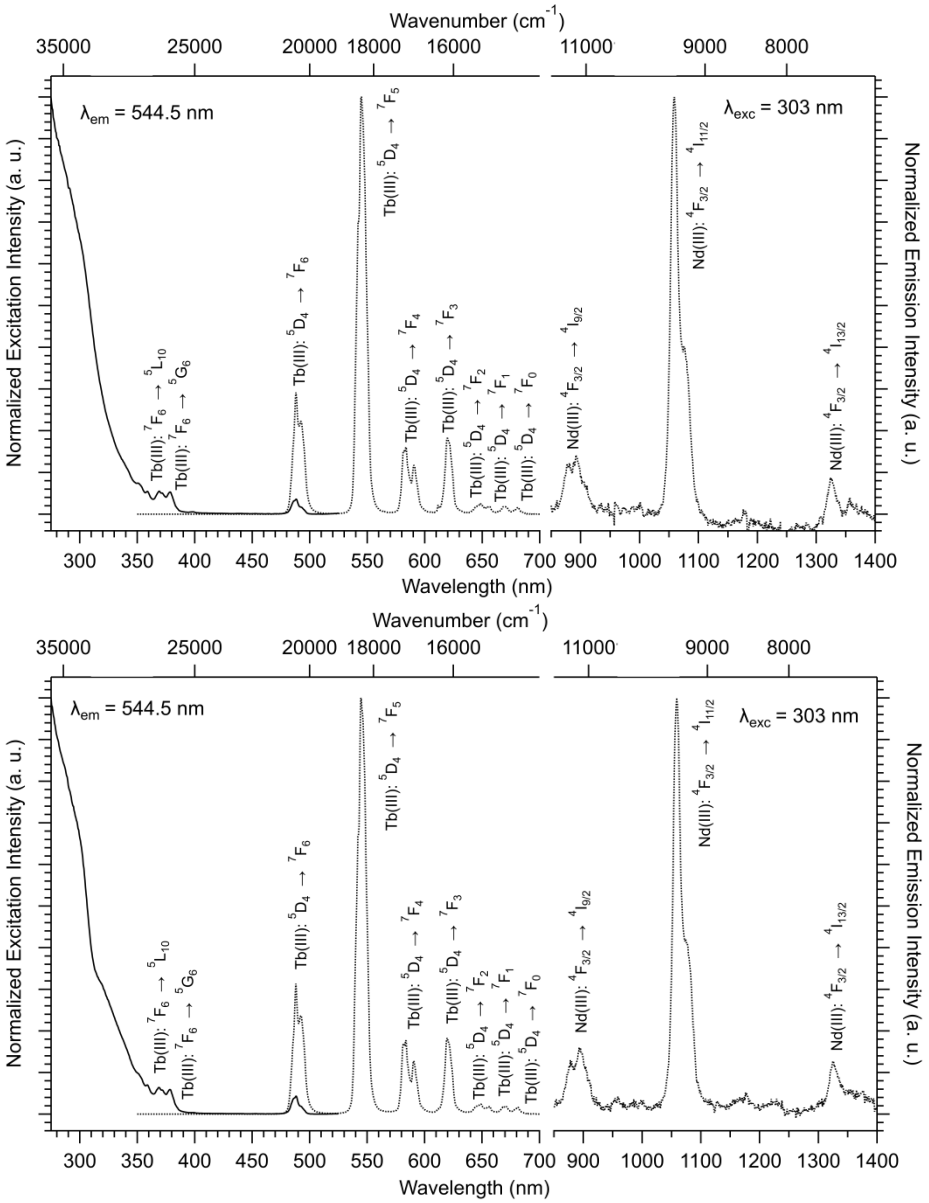

Figure 11. Solid state excitation and emission spectra of $[Tb_{0.95}Nd_{0.05}(cpbOH)]_\infty$ (Top) and of $[Gd_{0.2}Tb_{0.75}Nd_{0.05}(cpbOH)]_\infty$ (Bottom) at 293 K.

Luminescence lifetimes of the Tb^{3+} ion were measured for both compounds and inter-metallic energy transfer efficiency was calculated according to relationship **(1)**: η_{ET} = 34% for $[Tb_{0.95}Nd_{0.05}(cpbOH)]_\infty$ and 21% for $[Gd_{0.20}Tb_{0.75}Nd_{0.05}(cpbOH)]_\infty$ (Table 5).

These values evidences that dilution by Gd^{3+} ions strongly reduces the Tb^{3+}-to-Nd^{3+} intermetallic energy transfer.

Table 5. Luminescence lifetimes of the Tb^{3+} ion for $[Tb_{0.95}Gd_{0.05}(cpbOH))]_\infty$, $[Tb_{0.95}Nd_{0.05}(cpbOH)]_\infty$, $[Gd_{0.2}Tb_{0.8}(cpbOH)]_\infty$ and $[Gd_{0.2}Tb_{0.75}Nd_{0.05}(cpbOH)]_\infty$

Chemical formula	τ_{obs}(Tb) (ms)
$[Tb_{0.95}Gd_{0.05}(cpbOH)]_\infty$	0.86(1)
$[Tb_{0.95}Nd_{0.05}(cpbOH)]_\infty$	0.57(3)
$[Gd_{0.25}Tb_{0.75}(cpbOH)]_\infty$	0.85(1)
$[Gd_{0.20}Tb_{0.75}Nd_{0.05}(cpbOH)]_\infty$	0.67(1)

Additionally, in order to evaluate the Eu^{3+}-to-Nd^{3+} energy transfer, the series of compounds with general chemical formula $[Eu_{1-x}Nd_x(cpbOH)]_\infty$ with $0 \leq x \leq 1$ has been prepared. They are all isostructural to $[Tb(cpbOH)]_\infty$ (Figure S13 and Table S3). Their luminescent properties have been recorded (Figure 12)

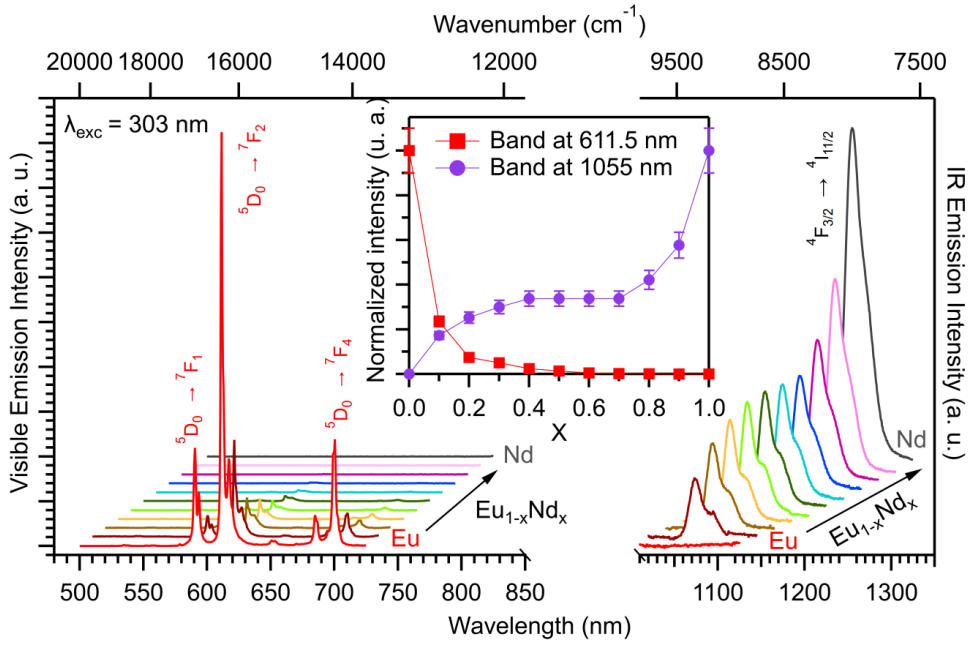

Figure 12. Luminescence spectra of $[Eu_{1-x}Nd_x(cpbOH)]_\infty$ with $0 \leq x \leq 1$ versus x (λ_{exc} = 303 nm) at 293 K. In inset, integrated intensities of the major characteristic emission peaks of Eu^{3+} and Nd^{3+} centered at 611.5 nm ($^5D_0 \rightarrow {}^7F_2$) and 1055 nm ($^4F_{3/2} \rightarrow {}^4I_{11/2}$) respectively versus x.

Figure 12 evidences a complex competition between energy transfer mechanisms. Indeed, Eu^{3+} luminescence abrutly decreases for $0 \leq x \leq 0.2$. This decreasing is accompagnied

by an increasing of Nd^{3+} luminescence. This is in agreement with an efficient Eu^{3+}-to-Nd^{3+} energy transfer. However for *x* values comprised between 0.2 and 0.8, Nd^{3+} luminescence is almost constant. Then it abruptly increases for *x* values comprised between 0.8 and 1. This behavior was unexpected and suggests a Nd^{3+}-to-Eu^{3+} energy back tranfer.

On the basis of these results, an isostructural hetero-lanthanide coordination polymer with chemical formula $[Gd_{0.20}Tb_{0.40}Eu_{0.25}Nd_{0.15}(cpbOH)]_\infty$ (Figure S14 and table S3) has been prepared and its solid state luminescent properties have been recorded (Figures 13 and S19).

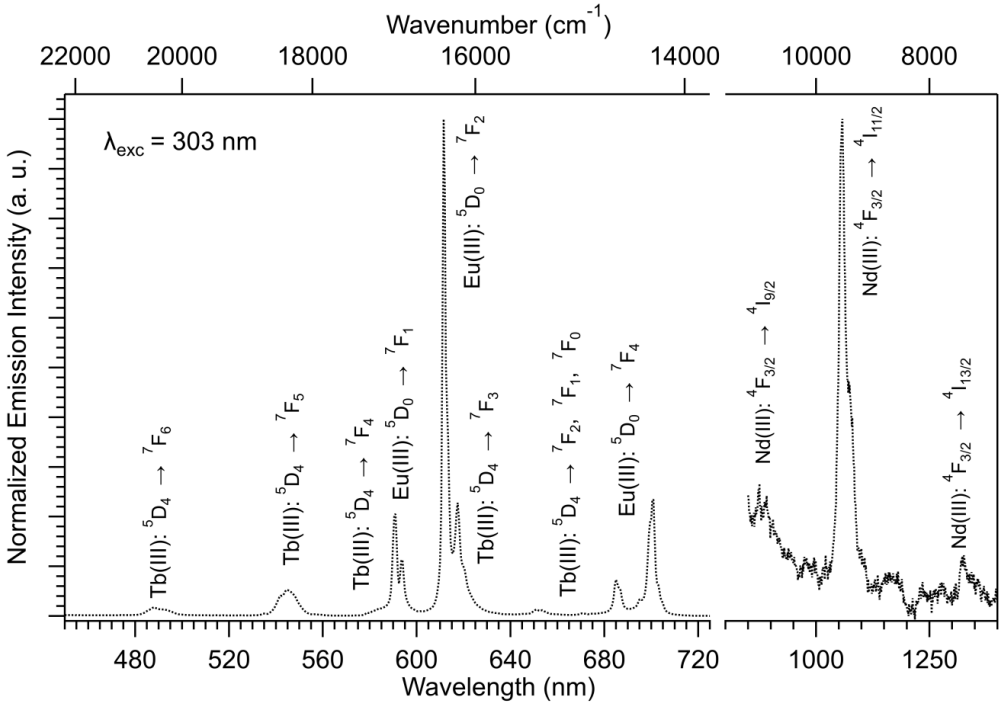

Figure 13. Solid state excitation and emission spectra of $[Gd_{0.20}Tb_{0.40}Eu_{0.25}Nd_{0.15}(cpbOH)]_\infty$ at 293 K. $\tau_{obs}(Tb) = 0.35(1)$ ms and $\tau_{obs}(Eu) = 0.17(1)$ ms at 293K.

As expected, this compound exhibits sizeable luminescence at room temperature in both the visible and the IR domains (Figure 13). Therefore, it should be possible to use this compound as a multi-gauge thermometer probe. In order to verify this assumption, luminescent properties have been measured in the range 77 K - 300 K in both visible and IR domains (Figure 14) and the two luminescence intensity ratios (I_{Tb}/I_{Eu} and I_{Tb}/I_{Nd}) have been extracted.

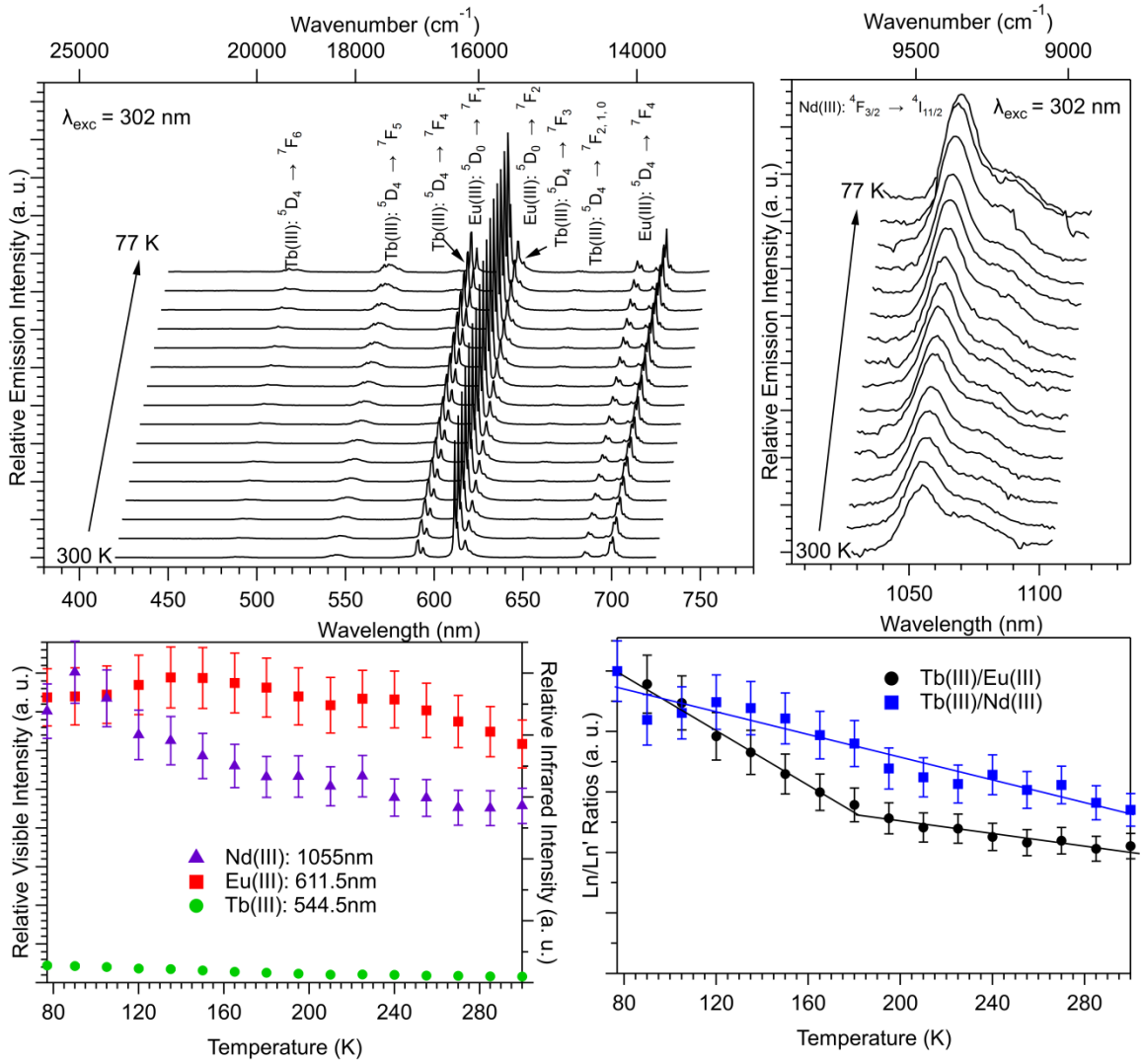

Figure 14. Solid state luminescence of $[Gd_{0.20}Tb_{0.40}Eu_{0.25}Nd_{0.15}(cpbOH)]_\infty$ *versus* temperature in both visible (Top left) and IR (Top right) regions in the 77 K - 300 K temperature range. Tb(III), Eu(III) and Nd(III) relative luminescence intensity (Bottom left) and luminescence intensity ratios (Bottom right) *versus* temperature between 77 K and 300 K. I_{Tb}/I_{Eu} *vs* T (Dark circles) and I_{Tb}/I_{Nd} *vs* T (Blue squares). τ_{obs}(Tb) = 0.45(1) ms and τ_{obs}(Eu) = 0.22(1) ms at 77 K.

On the basis of these measurements, it is possible to calculate the sensitivity toward temperature (from relationship (**3**)) of this compound in different temperature ranges (Table 6 and Figures S20 and S21).

Table 6. Luminescence of $[Gd_{0.20}Tb_{0.40}Eu_{0.25}Nd_{0.15}(cpbOH)]_\infty$ *versus* temperature. Linear function and thermometric sensitivities *vs* temperature range

$I_{Ln}/I_{Ln'}$	Linear function temperature range (K)	Linear function $T = f(I_{Ln}/I_{Ln'})$	Sensitivities temperature range (K)	Maximum sensitivities S (%.K^{-1})
I_{Tb}/I_{Eu}	77 - 180	-0.0045T + 1.3513 (R^2 = 0.99)	77 - 300	0.63 at 110 K
	180 - 300	-0.0011T + 0.7272 (R^2 = 0.89)		
I_{Tb}/I_{Nd}	77 - 300	-0.0018T + 1.0852 (R^2 = 0.92)	77 - 300	0.29 at 180 K

Table 6 evidences that multi-emissive materials can present different sensitivities in different temperature ranges. This could be of interest as far as accurate temperature measurements would be needed over a large temperature range or with host matrix that present dark optical zones.

It can also be noticed that comparison between figures 5, 9 10 and 14 evidences that in this system, inter-metallic energy transfer is strongly dependent of the temperature and the system composition (Figure 15).

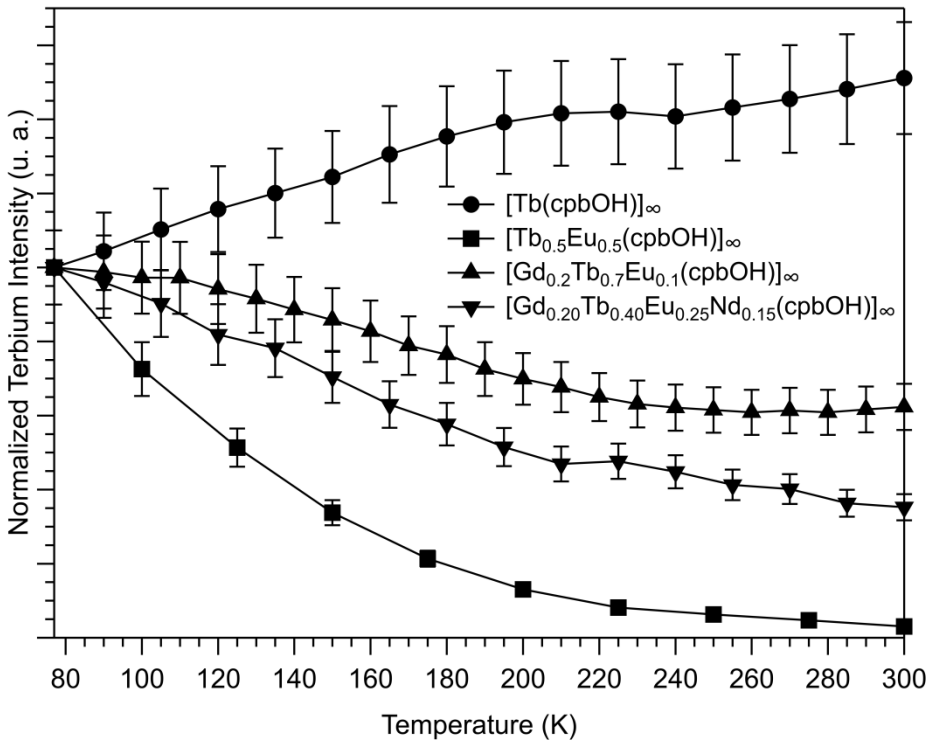

Figure 15. Tb(III) normalized luminescence intensities in $[Tb(cpbOH)]_\infty$, $[Tb_{0.5}Eu_{0.5}(cpbOH)]_\infty$, $[Gd_{0.2}Tb_{0.7}Eu_{0.1}(cpbOH)]_\infty$ and $[Gd_{0.20}Tb_{0.40}Eu_{0.25}Nd_{0.15}(cpbOH)]_\infty$.

CONCLUSIONS AND OUTLOOKS.

Compounds that are described in this paper present strong inter-metallic energy transfers and quite intense and temperature dependent emissions for Tb^{3+}, Eu^{3+} and Nd^{3+} ions.

The anisotropic nature of the metallic distribution in the material makes the optical dilution by Gd^{3+} ions efficient. Indeed, multiple emissions are achievable for 20% Gd^{3+} content. These results demonstrate that it is possible to modulate inter-metallic energy transfer and to design compounds that emit, under a unique excitation wavelength, in both visible and infra-red regions.

Efficiency of these not optimized compounds is far from the one exhibited by some previously reported systems.[28-29] However, to the best of our knowledge these compounds constitute the first example of potential multi-gauge thermometric probes based on multi-emission.[29]

ACKNOWLEDGEMENT.

The China Scholarship Council Ph.D. Program, a cooperation program with the French UT & INSA, is acknowledged for financial support.

SUPPORTING INFORMATION.

Crystal and final structure refinement data for Hcpb·0.25H_2O; Projection views of the asymmetric units and of the crystal packing of Hcpb·0.25H_2O; Experimental diagram of commercial Hcpb; TG/DSC analysis of Hcpb; TG/DSC analyses of Nacpb·1.5H_2O; Extended asymmetric unit of Nacpb·2H_2O; Crystal and final structure refinement data for Nacpb·2H_2O; Experimental powder X-ray diffraction diagrams of homo-lanthanide-based coordination polymers with 4-carboxyphenylboronic acid as ligand; Metallic relative contents in hetero-

lanthanide compounds; Experimental powder X-ray diffraction diagrams of $[Tb_{1-x}Gd_x(cpbOH)]_\infty$ with $0 \leq x \leq 1$, $[Eu_{1-x}Gd_x(cpbOH)]_\infty$ with $0 \leq x \leq 1$, $[Tb_{1-x}Eu_x(cpbOH)]_\infty$ with $0 \leq x \leq 1$, $[Gd_{0.2}Tb_{0.8-x}Eu_x(cpbOH)]_\infty$ with $0 \leq x \leq 1$, $[Gd_{0.20}Tb_{0.40}Eu_{0.25}Nd_{0.15}(cpbOH)]_\infty$, $[Gd_{0.20}Tb_{0.75}Nd_{0.05}(cpbOH)]_\infty$ and $[Tb_{0.95}Nd_{0.05}(cpbOH)]_\infty$, $[Eu_{1-x}Nd_x(cpbOH)]_\infty$ with $0 \leq x \leq 1$, $[Gd_{0.20}Tb_{0.40}Eu_{0.25}Nd_{0.15}(cpbOH)]_\infty$; Solid state excitation and emission spectra of $[Gd(cpbOH)]_\infty$ at 77 K; Solid state excitation and emission spectra of $[Ln(cpbOH)]_\infty$ with Ln = Sm(III), Dy(III) or Ho(III); Thermometric parameters calculations of $[Tb_{0.5}Eu_{0.5}(cpbOH)]_\infty$, $[Gd_{0.2}Tb_{0.7}Eu_{0.1}(cpbOH)]_\infty$ and $[Gd_{0.20}Tb_{0.40}Eu_{0.25}Nd_{0.15}(cpbOH)]_\infty$; Solid state emission spectra *vs* excitation wavelength (λ_{exc} = 295 - 400 nm) of $[Gd_{0.20}Tb_{0.40}Eu_{0.25}Nd_{0.15}(cpbOH)]_\infty$ at 293 K.

REFERENCES.

1. Alezi, D.; Peedikakkal, A. M. P.; Weselinski, L.; Guillerm, V.; Belmabkhout, Y.; Cairns, A. J.; Chen, Z.; Wojtas, L.; Eddaoudi, M., Quest for highly connected metal-organic framework platforms : rara earth polynuclear clusters versatility meets net topology needs. *J. Am. Chem. Soc.* **2015,** *137*, 5421-5430.
2. Guillerm, V.; Weselinski, L.; Belmabkhout, Y.; Cairns, A. J.; D'Elia, V.; Wojtas, L.; Adil, K.; Eddaoudi, M., Discovery and introduction of a (3,18)-connected net as an idel blueprint for the design of metal-organic frameworks. *Nat. Chem.* **2014,** *6*, 673-680.
3. Le Natur, F.; Calvez, G.; Freslon, S.; Daiguebonne, C.; Bernot, K.; Guillou, O., Extending the lanthanide terephthalate system : isolation of an unprecedented Tb(III)-based coordnation polmer with high potential porosity and luminescence properties. *J. Mol. Struc.* **2015,** *1086*, 34-42.
4. Luo, Y.; Bernot, K.; Calvez, G.; Freslon, S.; Daiguebonne, C.; Guillou, O.; Kerbellec, N.; Roisnel, T., 1,2,4,5-benzene-tetra-carboxylic acid : A versatile ligand for high dimensionnal lanthanide-based coordination polymers. *Cryst. Eng. Comm.* **2013,** *15*, 1882-1896.
5. Eddaoudi, M.; Kim, J.; Rosi, N.; Vodak, D.; Wachter, J.; O'Keeffe, M.; Yaghi, O. M., Systematic Design of Pore Size and Functionnality in Isoreticular MOFs and their application in Methane Storage. *Science* **2002,** *295*, 469-472.
6. Reneike, T. M.; Eddaoudi, M.; Fehr, M.; Kelley, D.; Yaghi, O. M., From Condensed Lanthanide Coordination Solids to Microporous Frameworks Having Accessible Metal sites. *J. Am. Chem. Soc.* **1999,** *121*, 1651-1657.
7. Kerbellec, N.; Daiguebonne, C.; Bernot, K.; Guillou, O.; Le Guillou, X., New lanthanide based coordination polymers with high potential porosity. *J. Alloys Compd.* **2008,** *451*, 377-383.
8. Devic, T.; Serre, C.; Audebrand, N.; Marrot, J.; Férey, G., MIL-103, A 3-D Lanthanide Based Metal Organic Framework with Large One Dimensionnal Tunnels and a High Surface area. *J. Am. Chem. Soc.* **2005,** *127*, 12788-12789.
9. Calvez, G.; Bernot, K.; Guillou, O.; Daiguebonne, C.; Caneschi, A.; Mahé, N., Sterically-induced synthesis of 3d-4f one-dimensional compounds: a new route towards 3d-4f Single Chain Magnets. *Inorg. Chim. Acta* **2008,** *361*, 3997-4003.
10. Bernot, K.; Luzon, J.; Caneschi, A.; Gatteschi, D.; Sessoli, R.; Bogani, L.; Vindigni, A.; Rettori, A.; Pini, M. G., Spin canting in a Dy-based single-chain magnet with dominant next-nearest-neighbor antiferromagnetic interactions. *Phys. Rev. B* **2009,** *79*, 134419 1-11.
11. Jeon, J. R.; Clérac, R., Controlled association of single-molecule magnets (SMMs) into coordination networks: towards a new generation of magnetic materials. *Dalton Trans.* **2012,** *41*, 9569-9586.
12. Cui, Y.; Li, B.; He, H.; Zhou, W.; Chen, B.; Qian, G., Metal-organic frameworks as platforms for functionnal materials. *Accounts Chem. Res.* **2016,** *49*, 483-493.
13. Li, B.; Wen, H.-M.; Cui, Y.; Qian, G.; Chen, B., Multifunctionnal lanthanide coordination polymers. *Prog. Polym. Sci.* **2015,** *48*, 40-84.
14. Bünzli, J. C. G., On the design of highly luminescent lanthanide complexes. *Coord. Chem. Rev.* **2015,** *293-294*, 19-47.
15. Cui, Y.; Zhang, J.; He, H.; Qian, G., Photonic functional metal–organic frameworks. *Chem. Soc. Rev.* **2018,** *47*, 5740-5785.
16. Bünzli, J. C. G., Rising stars in science and technology : Luminescent lanthanide materials. *Eur. J. Inorg. Chem.* **2017**, 5058-5063.
17. Li, X.-Y.; Shi, W.-J.; Wang, X.-Q.; Ma, L.-N.; Hou, L.; Wang, Y.-Y., Luminescence modulation, white light emission and energy transfer in a family of lanthanide Metal-Organic Frameworks based on a planar π-conjugated ligand. *Cryst. Growth Des.* **2017,** *17*, 4217-4224.
18. Dang, S.; Min, X.; Yang, W.; Yi, F. Y.; You, H.; Sun, Z. M., Lanthanide metal-organic frameworks showing luminescence in the visible and near infrared regions with potential for acetone sensing. *Chem. - Eur. J.* **2013,** *19*, 17172-17179.

19. Guillou, O.; Daiguebonne, C.; Calvez, G.; Bernot, K., A long journey in lanthanide chemistry : from fundamental crystallogenesis studies to commercial anti-counterfeiting taggants. *Accounts Chem. Res.* **2016,** *49*, 844-856.
20. Yang, Q. Y.; Pan, M.; Wei, S. C.; Li, K.; Du, B. B.; Su, C. Y., Linear dependance of photomuminescence in mixed Ln-MOFs for color tunability and barcode application. *Inorg. Chem.* **2015,** *54*, 5707-5716.
21. Andres, J.; Hersch, R. D.; Moser, J. E.; Chauvin, A. S., A new counterfeiting feature relying on invisible luminescent full color images printed with lanthanide-based Inks. *Adv. Func. Mater.* **2014,** *24*, 5029-5036.
22. Rao, X.; Song, T.; Gao, J.; Cui, Y.; Yang, Y.; Wu, C.; Chen, B.; Qian, G., A highly sensitive mixed lanthanide metal organic framework self calibrated luminescent thermometer. *J. Am. Chem. Soc.* **2013,** *135*, 15559-15564.
23. Cui, Y.; Xu, H.; Yue, Y.; Guo, Z.; Yu, J.; Chen, Z.; Gao, J.; Yang, Y.; Qian, G.; Chen, B., A Luminescent Mixed-Lanthanide Metal-Organic Framework Thermometer. *J. Am. Chem. Soc.* **2012,** *134*, 3979-3982.
24. Cui, Y.; Zou, W.; Song, R.; Yu, J.; Zhang, W.; Yang, Y.; Qian, G., A ratiometric and colorimetric luminescent thermometer over a wide temperature range based on a lanthanide coordination polymer. *Chem. Comm.* **2014,** *50*, 719-721.
25. Cui, Y.; Sog, R.; Yu, J.; liu, M.; Wang, Z.; Wu, C.; Yang, Y.; Wang, Z.; Chen, B.; Qian, G., Dual emitting MOF-Dye composite for ratiometric temperature sensing. *Adv. Mater.* **2015,** *27*, 1420-1425.
26. Cadiau, A.; Brites, D. S. C.; Costa, P. M. F. J.; Ferreira, R. A. S.; Rocha, J.; Carlos, L. D., Ratiometric nanomether based on an emissive Ln^{3+}-organic framework. *ACS Nano* **2013,** *7*, 7213-7218.
27. Chuasaard, T.; Ngamjarurojana, A.; Surinwong, S.; Konno, T.; Bureekaew, S.; Rujiwatra, A., Lanthanide coordination polymers of mixed phthalate/adipate for ratiometric temperature sensing in the upper-intermediate temperature range. *Inorg. Chem.* **2018,** *57*, 2620-2630.
28. Brites, D. S. C.; Lima, P. P.; Silva, N. J. O.; Millan, A.; Amaral, V. S.; Palacio, F.; Carlos, L. D., Lanthanide-based luminescent molecular thermometers. *New J. Chem.* **2011,** *35*, 1177-1183.
29. Rocha, J.; Brites, D. S. C.; Carlos, L. D., Lanthanide organic framework luminescent thermometers. *Chem. - Eur. J.* **2016,** *22*, 14782-14795.
30. Zhou, J.; Li, H.; Zhang, H.; Li, H.; Shi, W.; Cheng, P., A bimetallic lanthanide metal-organic material as a self-calibrating color-gradient luminescent sensor. *Adv. Mater.* **2015,** *27*, 7072-7077.
31. Ren, M.; Brites, D. S. C.; Bao, S.-S.; Ferreira, R. A. S.; Zheng, L.-M.; Carlos, L. D., A cryogenic luminescent ratiometric thermometer based on lanthanide phosphonate dimer. *J. Mater. Chem. C* **2015,** *3*, 8480-8484.
32. Wang, K.-M.; Du, L.; Ma, Y.-L.; Zhao, J.-S.; Wang, Q.; Yan, T.; Zhao, Q.-H., Multifunctionnal chemical sensors and luminescent thermometers based on lanthanide metal-organic framework materials. *Cryst. Eng. Comm.* **2016,** *18*, 2690-2700.
33. An, R.; Zhao, H.; Hu, H.-M.; Wang, X.; Yang, M.-L.; Xue, G., Synthesis, structure, white light emission and temperature recognition properties of Eu/Tb mixed coordination polymers. *Inorg. Chem.* **2016,** *55*, 871-876.
34. Yang, Y.; Chen, L.; Jiang, F.; Yu, M.; Wan, X.; Zhang, B.; Hong, M., A family of doped lanthanide metal organic frameworks for wide-range temperature sensing and tunable white light emission. *J. Mater. Chem. C* **2017,** *5*, 1981-1989.
35. Zhou, X.; Chen, L.; Feng, L.; Jiang, S.; Lin, J.; Pang, Y.; Li, L.; Xiang, G., Color tunable emission and low-temperature luminescent sensing of europium and terbium carboxylic acid complexes. *Inorg. Chim. Acta* **2018,** *469*, 576-582.
36. Khudoleeva, V.; Tcelykh, L.; Kovalenko, A.; Kalyakina, A.; Goloveshkin, A.; Lepnev, L. S.; Utochnikova, V., Terbium-europium fluorides surface modified with benzoate and terephthalate anions for temperature sensing : Does sensitivity depends on the ligand ? *J. Lumin.* **2018,** *201*, 500-508.

37. Song, X.-Q.; Zhang, M.-L.; Wang, C.-Y.; Shamshooma, A. A. A.; Meng, H.-H.; Xi, W., Mixed lanthanide coordination polymers for temperature sensing and enhanced Nd^{III} NIR luminescence. *J. Lumin.* **2018,** *201*, 410-418.
38. Zhou, D.; Huang, C.; Wang, K.; Xu, G., Synthesis, characterization, crystal structure and luminescent property studies on a novel heteronuclear lanthanide complex $\{H[EuLa_2(DPA)_5.8H_2O].8H_2O\}_n$ (H_2DPA=pyridine-2,6-dicarboxylic acid). *Polyhedron* **1994,** *13*, 987-991.
39. Badiane, I.; Freslon, S.; Suffren, Y.; Daiguebonne, C.; Calvez, G.; Bernot, K.; Camara, M.; Guillou, O., High britness and easy color modulation in lanthanide-based coordination polymers with 5-methoxyisophthalate as ligand: Toward emission colors additive strategy. *Cryst. Growth Des.* **2017,** *17*, 1224-1234.
40. Freslon, S.; Luo, Y.; Daiguebonne, C.; Calvez, G.; Bernot, K.; Guillou, O., Brightness and color tuning in a series of lanthanide-based coordination polymers with benzene 1,2,4,5-tetracarboxylic acid as ligand. *Inorg. Chem.* **2016,** *55*, 794-802.
41. Freslon, S.; Luo, Y.; Calvez, G.; Daiguebonne, C.; Guillou, O.; Bernot, K.; Michel, V.; Fan, X., Influence of photo-induced electron transfer on lanthanide-based coordination polymers luminescence : A comparison between two pseudo-isoreticular molecular networks. *Inorg. Chem.* **2014,** *53*, 1217-1228.
42. Fan, X.; Freslon, S.; Daiguebonne, C.; Calvez, G.; Le Polles, L.; Bernot, K.; Guillou, O., Heteronuclear lanthanide-based coordination polymers exhibiting tunable multiple emission spectra. *J. Mater. Chem. C* **2014**, 5510-5525.
43. Haquin, V.; Etienne, M.; Daiguebonne, C.; Freslon, S.; Calvez, G.; Bernot, K.; Le Polles, L.; Ashbrook, S. E.; Mitchell, M. R.; Bünzli, J. C. G.; Guillou, O., Color and Brightness tuning in hetero-nuclear lanthanide teraphthalate coordination polymers. *Eur. J. Inorg. Chem.* **2013**, 3464-3476.
44. Badiane, A. M.; Freslon, S.; Daiguebonne, C.; Suffren, Y.; Bernot, K.; Calvez, G.; Costuas, K.; Camara, M.; Guillou, O., Lanthanide based coordination polymers with a 4,5-dichlorophthalate ligand exhibiting highly tunable luminescence : Toward luminescent bar codes. *Inorg. Chem.* **2018,** *57*, 3399-3410.
45. Hall, D. G., *Boronic acids*. Wiley-VCH Verlag: Weinheim, 2005.
46. Sene, S.; Pizzoccaro, M. A.; Vezzani, J.; Reinholdt, M.; Gaveau, P.; Berthomieu, D.; Bégu, S.; Gervais, C.; Bonhomme, C.; Renaudin, G.; Mesbah, A.; van der Lee, A.; Smith, M. E.; Laurencin, D., Coordination networks based on boronate and benzoxaborolate ligands. *Crystals* **2016,** *6*, 48-61.
47. Lekshmi, N. S.; Pedireddi, V. R., First study of metal hybrids of boronic acis : Second sphere coordination networks in the structures of 4-carboxyphenylboronic acid with some transition metal ions. *Inorg. Chem.* **2006,** *45*, 2400-2402.
48. Fan, X.; Freslon, S.; Daiguebonne, C.; Le Polles, L.; Calvez, G.; Bernot, K.; Guillou, O., A family of lanthanide based coordination polymers with boronic acid as ligand. *Inorg. Chem.* **2015,** *54*, 5534-5546.
49. Yang, Z.-R.; Wang, M.-M.; Wang, X.-S.; Yin, X.-B., Boric acid functional lanthanide metal organic frameworks for selective ratiometric fluorescence detaction of fluoride ions. *Anal. Chem.* **2016,** *89*, 1930-1936.
50. Lekshmi, N. S.; Pedireddi, V. R., Solid state structure of 4-carboxyphenylboronic acid and its hydrates. *Cryst. Growth Des.* **2007,** *7*, 944-949.
51. Desreux, J. F., In *Lanthanide Probes in Life, Chemical and Earth Sciences*, Choppin, G. R.; Bünzli, J. C. G., Eds. Elsevier: Amsterdam, 1989; Vol. Elsevier, p 43.
52. Le Natur, F.; Calvez, G.; Daiguebonne, C.; Guillou, O.; Bernot, K.; Ledoux, J.; Le Polles, L.; Roiland, C., Coordination polymers based on hexanuclear rare earth complexes : Toward independant luminescence brightness and color emission. *Inorg. Chem.* **2013,** *52*, 6720-6730.
53. Henisch, H. K., *Crystals in Gels and Liesegang Rings*. Cambridge University Press: Cambridge, 1988.
54. Henisch, H. K.; Rustum, R., *Crystal Growth in Gels*. The Pennsylvania State University Press: 1970; p 1-196.

55. Daiguebonne, C.; Deluzet, A.; Camara, M.; Boubekeur, K.; Audebrand, N.; Gérault, Y.; Baux, C.; Guillou, O., Lanthanide-based molecular materials : gel medium induced polymorphism. *Cryst. Growth Des.* **2003,** *3*, 1015-1020.
56. Altomare, A.; Burla, M. C.; Camalli, M.; Carrozzini, B.; Cascarano, G.; Giacovazzo, C.; Guagliardi, A.; Moliterni, A. G. G.; Polidori, G.; Rizzi, A. C., EXPO: a program for full powder pattern decomposition and crystal structure solution. *J. Appl. Crystallogr.* **1999,** *32*, 339-340.
57. Sheldrick, G. M.; Schneider, T. R., SHELXL : High-Resolution Refinement. *Macromol. Crystallogr. B* **1997**, 319-343.
58. Farrugia, L. J., WinGX suite for smallmolecule single-crystal crystallography. *J. Appl. Crystallogr.* **1999,** *32*, 837-838.
59. Sluis, P.; Spek, A. L., BYPASS: an Effective Method for the Refinement of Crystal Structures Containing Disordered Solvent Regions. *Acta Crystallogr. A* **1990,** *A46*, 194-201.
60. Kraus, W.; Nolze, G., POWDER CELL - A program for the representation and manipulation of crystal structures and calculation of the resulting X-ray powder patterns. *J. Appl. Crystallogr.* **1996,** *29*, 301-303.
61. Roisnel, T.; Rodriguez-Carjaval, J., A Window Tool for Powder Diffraction Patterns Analysis. *J. Mater. Sci. Forum* **2001,** *378*, 118-123.
62. Roisnel, T.; Rodriguez-Carjaval, J., WinPLOTR : a windows tool for powder diffraction pattern analysis. *Materials Science Forum, Proceedings of the Seventh European Powder Diffraction Conference (EPDIC 7)* **2000**, 118-123.
63. CIE, *International Commission on Illumination - Technical report*. CIE: 1995; Vol. 13-3, p 16.
64. Wyszecki, G., Colorimetry. In *Handbook of Optics*, Driscoll, W. G.; Vaughan, W., Eds. Mac Graw-Hill Book Company: New-York, 1978; pp 1-15.
65. Luo, Y.; Zheng, Y.; Calvez, G.; Freslon, S.; Bernot, K.; Daiguebonne, C.; Roisnel, T.; Guillou, O., Synthesis, Crystal Structure and Luminescent Properties of New Lanthanide-Containing Coordination Polymers Involving 4,4'-oxy-bis-benzoate as Ligand. *Cryst. Eng. Comm.* **2013,** *15*, 706-720.
66. Dexter, D. L., A theory of sensitized luminescence in solids. *J. Chem. Phys.* **1953,** *21*, 836-850.
67. Förster, T., *Comparative effects of radiation*. John Wiley & Sons: New-York, 1960.
68. Shi, M.; Li, F.; Yi, T.; Zhang, D.; Hu, H.; Huang, C.-H., Tuning the Triplet Energy Levels of Pyrazolone Ligands to Match the $^5D_0$ Level of Europium(III). *Inorg. Chem.* **2005,** *44*, 8929.
69. Prodi, L.; Maestri, M.; Ziessel, R.; Balzani, V., Luminescent Eu3+, Tb3+ and Gd3+ complexes of a branched triazacyclononane ligand containing three 2,2'bipyridine units. *Inorg. Chem.* **1991,** *30*, 3798-3802.
70. Bünzli, J. C. G.; Eliseeva, S. V., Basics of lanthanide photophysics. In *Lanthanide Luminescence*, Hänninen, P.; Härmä, H., Eds. Springer Berlin Heidelberg: 2010; pp 1-45.
71. Steemers, F. J.; Verboom, W.; Reinhoudt, D. N.; Van der Tol, E. B.; Verhoeven, J. W., New sensitizer-modified calix[4]arenes enabling Near-UV Excitation of complexed luminescent lanthanide ions. *J. Am. Chem. Soc.* **1995,** *117*, 9408-9414.
72. Weissman, S. I., Intramolecular energy transfer - The fluorescence of complexes of europium. *J. Chem Phys* **1942,** *10*, 214-217.
73. Latva, M.; Takalo, H.; Mukkala, V.-M.; Matachescu, C.; Rodriguez-Ubis, J. C.; Kankare, J., Correlation between the lowest triplet state energy level of the ligand and lanthanide luminescence quantum yields. *J. Lumin.* **1997,** *75*, 149-169.
74. Eliseeva, S. V.; Bünzli, J. C. G., Lanthanide luminescence for functionnal materials and bio-sciences. *Chem. Soc. Rev.* **2010,** *39*, 189-227.
75. Lannes, A.; Intissar, M.; Suffren, Y.; Reber, C.; Luneau, D., Terbium(III) and yttrium(III) complexes with pyridine-substituted nitronyl nitroxide radical and different beta-diketonate ligands. Crystal structures and magnetic and luminescence properties. *Inorg. Chem.* **2014,** *53*, 9548-9560.
76. Le Natur, F.; Calvez, G.; Guéguan, J. P.; Le Polles, L.; Trivelli, X.; Bernot, K.; Daiguebonne, C.; Neaime, C.; Costuas, K.; Grasset, F.; Guillou, O., Characterization and luminescence properties of lanthanide based polynuclear complexes nanoaggregates. *Inorg. Chem.* **2015,** *54*, 6043-6054.

77. Rodrigues, M. O.; Dutra, J. D. L.; Nunes, L. A. O.; de Sa, G. F.; de Azevedo, W. M.; Silva, P.; Paz, F. A. A.; Freire, R. O.; Junior, S. A., Tb3+->Eu3+ energy transferin mixed lanthanide organic frameworks. *J. Phys. Chem. C* **2012,** *116*, 19951-19957.

TABLE OF CONTENT GRAPHIC.

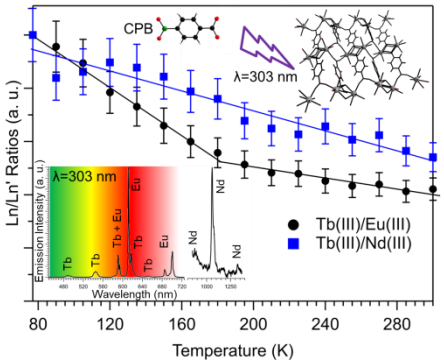

TABLE OF CONTENT.

Reactions in water of lanthanide chlorides with the sodium salt of 1,4-carboxyphenyl boronic acid lead to multi-emissive lanthanide-based coordination polymers that could find their application as multi-gauge luminescent thermometric probes.